1

2 **Stepwise progression of β-selection during T cell development as revealed by histone**

3 **deacetylation inhibition**

4 **TCR co-receptors are expressed sequentially to fine-tune early αβ T cell development**

5 [1,2,3,9]Anchi S Chann, [1,2]Mirren Charnley, [4]Lucas M. Newton, [2,5]Andrea Newbold, [3,9] Florian Wiede, [3,9]

6 Tony Tiganis, [4,6,7,8]Patrick O Humbert, [2,5]Ricky W Johnstone, [1,2,5]Sarah M Russell.

7 **Affiliations**

8 [1]Optical Sciences Centre, School of Science, Swinburne University of Technology, Hawthorn, Victoria

9 3122, Australia.

10 [2]Peter MacCallum Cancer Centre, Melbourne, Victoria 3000, Australia.

11 [3]Monash Biomedicine Discovery Institute, Monash University, Clayton, Victoria 3800, Australia.

12 [4] Department of Biochemistry & Chemistry, La Trobe Institute for Molecular Science, La Trobe

13 University, Melbourne, Victoria 3086, Australia.

14 [5]Sir Peter MacCallum Department of Oncology, The University of Melbourne, Victoria 3010, Australia.

15 [6] Research Centre for Molecular Cancer Prevention, La Trobe University, Melbourne, Victoria 3086,

16 Australia.

17 [7]Department of Biochemistry & Pharmacology, University of Melbourne, Melbourne, Victoria 3010,

18 Australia.

19 [8]Department of Clinical Pathology, University of Melbourne, Melbourne, Victoria 3010, Australia.

20 [9]Department of Biochemistry and Molecular Biology, Monash University, Clayton, Victoria 3800,

21 Australia.

22

23

24 *To whom correspondence should be addressed: Sarah Russell: sarah.russell@petermac.org;

25 613-433-354-996; Optical Sciences Centre, School of Science, Hawthorn, Australia

26

27 ORCID ID: 0000-0002-8778-5327 (ASC); ORCID ID: 0000-0003-3845-9290 (MC); ORCID

28 ID: 0000-0002-1366-6691(POH); 0000-0001-5826-9641 (SMR); 0000-0001-7053-9237

29 (RWJ); 0000-0002-0481-2431 (AN); 0000-0001-5984-5778 (LMN); 0000-0001-5145-7180

30 (FW);

31

Abstract

During T cell development, the first step in creating a unique T Cell Receptor (TCR) is the genetic recombination of the TCRβ chain. The quality of the newly recombined TCRβ is assessed at the β-selection checkpoint. Most cells fail this checkpoint and die, but the coordination of the complex events that control fate at the β-selection checkpoint is not yet understood. We shed new light on fate determination during β-selection using a selective inhibitor of histone deacetylase 6, ACY1215. ACY1215 disrupted the β-selection checkpoint. Characterising the basis for this disruption revealed a new, pivotal stage in β-selection, bookended by upregulation of the TCR co-receptors, CD28 and CD2 respectively. Within this 'DN3b^{Pre}' stage, CD5 and Lef1 are upregulated to reflect pre-TCR signalling and their expression correlates with proliferation. During this phase, ACY1215-mediated disruption of the organisation of the β-selection immunological synapse is associated with a breakdown in connectivity of expression of pre-TCR, CD5 and Lef1. Subsequent deregulation of pre-TCR-induced proliferation leads to bypass of the β-selection checkpoint and subsequent failure to progress. We propose that the progressive expression of CD28, CD5 and Lef1, then CD2 reports and modulates the pre-TCR signal to orchestrate passage through the β-selection checkpoint. These findings suggest a refined model of β-selection in which a coordinated increase in expression of pre-TCR, CD28, CD5 and Lef1 allows for modulating TCR signalling strength, and culminates in the expression of CD2 to enable exit from the β-selection checkpoint.

Introduction

T cells are generated in a multistep, highly orchestrated process guided by stromal cells in the thymus. T cell development involves massive cell proliferation interspersed with genomic recombination of the T cell receptor (TCR). If genomic recombination, proliferation and death are not appropriately orchestrated, the implications for cancer and immunity are profound. Uncontrolled self-renewal or a sub-optimal TCR repertoire can lead to T cell acute lymphoblastic lymphoma (T-ALL), autoimmunity or limited response to pathogens or cancers (Ballesteros-Arias et al., 2019; Douek et al., 2000; Notarangelo et al., 2020). T cell development is most tightly controlled during genomic recombination to generate the TCR. For the most common αβ T cells, the β chain is generated at the

59 DN3a phase of T cell development (see **Supp Fig 1A** for a description of T cell development and the
60 surface markers by which it is assessed), and the appropriateness of this TCRβ sequence is assessed
61 during the β-selection checkpoint. During β-selection, the strength of the TCRβ chain is tested in
62 combination with a surrogate 'pre-TCR' before the TCRα chain is created (Chann and Russell, 2019;
63 Dutta et al., 2021).

64 β-selection is in part determined by stromal cells in the thymic microenvironment, which provide
65 Notch and chemokine signals that promote survival and differentiation (Chann and Russell, 2019;
66 Dutta et al., 2021). Recently, it has become clear that interactions between the pre-TCR and the
67 MHC-peptide on stromal cells also provide an opportunity to test TCR signalling (Allam et al., 2021;
68 Dutta et al., 2021; Li et al., 2021) These interactions trigger a sequence of transcriptional changes and
69 epigenetic modifications that ensure only the cells with an appropriately recombined TCRβ chain
70 survive, proliferate and differentiate. How pre-TCR signalling integrates fate determination including
71 proliferation, differentiation and survival during β-selection is still not understood (Chann and
72 Russell, 2019; Dutta et al., 2021).

73 Epigenetic therapies such as small-molecule inhibitors of histone deacetylases (HDAC) have shown
74 great promise in mediating clinical antitumor responses and are emerging as immune modulators
75 (Hogg et al., 2020). The HDAC6 selective inhibitor ACY1215 (Ricolinostat) can synergize with the
76 BET inhibitor, JQ1, to recruit T cell mediated responses to lung adenocarcinoma, enhance T cell
77 responses to *ex vivo* melanoma cultures, impair effector CD8 T cell function during skin
78 inflammation, and alter Treg function (Adeegbe et al., 2017; Laino et al., 2019; Tsuji et al., 2015; Xu
79 et al., 2018; Zhang et al., 2021). HDACs 1, 2, and 3 are required at multiple stages of T cell
80 development, but a role for HDAC6 in T cell development has not been identified (Wang et al., 2020).
81 Mice lacking HDAC6 showed no overt T cell phenotypes (Shapiro and Shapiro, 2020; Zhang et al.,
82 2008) and to our knowledge the effect of acute deletion of HDAC6, or pharmacological inhibition of
83 HDAC6 on T cell development has not been reported (Shapiro and Shapiro, 2020). Here, we show a
84 striking effect of treatment with the HDAC6-selective inhibitor, ACY1215, on β-selection.

85 This effect of ACY1215 allowed us to define several stages of β-selection with high resolution. After
86 the DN3a stage marked by upregulation of the co-receptor, CD28, we observed a transitional stage
87 marked by low levels of the co-receptor, CD2, that we termed DN3b^{Pre}. DN3b^{Pre} cells are enriched by
88 ACY1215 treatment. An upregulation of CD2 marks passage through the β-selection checkpoint, to a
89 phase we termed DN3b^{Post}. The transcription factor, Lef1 is upregulated in DN3b^{Pre} cells, together
90 with an increasing expression of the reporter of TCR signalling, CD5. These findings implicate a
91 refined model of β-selection in which, following expression of CD27 and CD28, a coordinated
92 increase in expression of pre-TCR, CD5 and Lef1 provides for an escalating test of TCR signalling.
93 Expression of CD2 marks the passing of this test and exit from the β-selection checkpoint.

94

95 **Results**

96 **Treatment with ACY1215 impairs T cell differentiation at the β-selection stage.**

97 To examine the effects of ACY1215 on T cell development **(Supp Fig 1A, B)**, we used two models.
98 Firstly, a well validated *in vitro* model in which hematopoietic stem cells extracted from mouse fetal
99 liver were co-cultured with the OP9 mouse bone marrow stromal cell line transfected with the Notch
100 ligand, DL1 ('OP9-DL1') (Holmes and Zúñiga-Pflücker, 2009). To assess relevance of our findings to
101 physiological T cell development in the thymus, we also analysed cells directly taken from young
102 adult mice.

103 At Day 8-10 of the co-culture, when DN cells from mouse fetal liver were predominantly at the DN3
104 stage of T cell development **(Supp Fig 1B)**, we applied the HDAC6 inhibitor, ACY1215 at a
105 concentration previously reported to alter function of mature T cells without affecting lymphocyte
106 viability (Laino et al., 2019). Compared with DMSO-treated cells, cells treated with ACY1215 for
107 two days (**Figure 1A**) showed reduced proportions of the later stages of differentiation, suggesting
108 HDAC6 is required for optimal T cell development to the DP stage. The impact was directly on the T
109 cells, since ACY1215 had no effect on growth or acetylation of tubulin in the OP9-DL1 stromal cells
110 (Supp Fig 2A, 2B), and ACY1215-treated stromal cells provided proper spport for thymocyte

111 attachment and differentiation (**Supp Fig2**B, C), The shift in differentiation caused by ACY1215 was
112 accompanied by a generalised inhibition of expansion in cell numbers at several stages of T cell
113 development (Supp Fig **2D**). Comparing proportions at different DN stages using CD25 and CD44
114 expression (Figure 1A) showed an increase in the proportions of DN3 cells and commensurate
115 decrease in proportions of DN4, suggesting that the ACY1215-treated cells were blocked at the DN3
116 stage.

117 The DN3 stage incorporates the β-selection checkpoint. The passing of the β-selection checkpoint,
118 conventionally conceptualised as DN3a-to-DN3b progression, is marked by the expression of CD28
119 (Teague et al., 2010; Williams et al., 2005). Therefore, we assessed whetherDN3a (DN3, $CD28^{Lo}$)
120 cells were inhibited from progressing to DN3b (DN3, $CD28^{Hi}$) by ACY1215 treatment over one and
121 two days (**Figure 1B**). Surprisingly, the reverse was observed. Co-staining with CD25 and CD28
122 indicated a relatively stable distribution between DN3a and DN3b at 1 and 2 days in the control
123 cultures, but increasingly greater proportions of DN3b cells in the ACY1215-treated cultures. A
124 similar shift to DN3b and DN4 at the expense of DN3a was observed in thymocytes extracted from an
125 adult mouse and cultured for 1 day on OP9-DL1, although the relatively low numbers of DN3a in
126 primary thymocytes *ex vivo* (**Supp Fig 1C)** made the shift less obvious (**Figure 1C**).

127 We explored the cellular basis of this shift away from DN3a towards DN3b. Cell counts of cultures of
128 sorted DN3a cells showed that the DN3a cells expanded more than 4-fold over 2 days of control
129 DMSO-treated culture, but this was dramatically reduced by ACY1215 treatment (Fig 1B**)**. In
130 contrast, ACY1215 caused a negligible reduction in absolute numbers of DN3b and DN4 cells arising
131 from DN3a. This stage-specific effect was probably not due to differences in proliferation or death
132 because CFSE and Ki-67 labelling showed similar inhibition of proliferation of DN3a and DN3b cells
133 (**Supp Fig 3**) and neither DN3a or DN3b cells were demonstrably susceptible to cell death, although
134 DP cells died more in the presence of ACY1215 (**Supp Fig 4**). Together, these data suggest that
135 ACY1215 treatment of DN3a cells led to reduced amplification, but little impact or a compensatory
136 increase in the number of cells passing through the DN3b stage.

137 To reconcile the seemingly normal progression through β-selection (as indicated by DN3b and DN4
138 counts) with the block in DP cells, we first monitored differentiation from sorted DN3a and DN3b
139 cells that had been treated for four days with ACY1215 or DMSO (**Supp Fig 5**). Progression past the
140 DN3 stages was inhibited for both DN3a and DN3b starting populations, although less clear for the
141 DN3a starting population due to limited differentiation by Day 4. To confirm that the effect at β-
142 selection led to a downstream impact on DP cells, we counted the number of cells at each
143 differentiation stage that developed from the sorted DN3b population (**Figure 1D**). By day 4, DN3b
144 cells had expanded more than 50-fold, with a negligible reduction caused by treatment with
145 ACY1215. DN4 cell numbers were also only slightly reduced by ACY1215 treatment, but DP were
146 reduced by over two orders of magnitude. These data together suggest that ACY1215 treatment
147 impacts generally upon cell expansion, but also alters differentiation to DP by acting at the DN3
148 stage, perhaps by causing precocious differentiation from DN3a to DN3b.

149 The DN3 cell stage involves fate choice between two T cell lineages (αβ cells and γδ cells), each
150 expressing a different set of T cell receptors (Hayday and Pennington, 2007). To determine which
151 lineage was altered by ACY1215, we cultured developing T cells for 2 days with and without
152 HDAC6i and labelled the cells with antibodies specific for these TCRs to assess progression through
153 the DN and DP stages (**Supp Fig 6**). ACY1215 treatment reduced the proportion of TCRβ–expressing
154 cells at all stages following β-selection but did not inhibit TCRγδ development. Together, these data
155 indicated that the defect in differentiation to DP following ACY1215 treatment was specific to αβ T
156 cells, and likely involved the β-selection checkpoint.

157 One possible explanation for this passage to DN3b without optimal subsequent differentiation could
158 be that ACY1215-treated cells express some markers suggestive of differentiation, but are not
159 competent precursors of αβ T cells. To assess this, we first characterised several phenotypic markers
160 implicated in progression through the β-selection checkpoint. Co-staining DN3 cells with both CD28
161 and CD27, both of which can discriminate between DN3a and DN3b cells (Taghon et al., 2006;
162 Teague et al., 2010) clearly discriminated two subpopulations in DN3 cells pre-treated with DMSO
163 (**Figure 2A**). A shift from DN3a to DN3b is observed for both fetal liver-derived lymphocytes and *ex*

164 *vivo* extracted thymocytes cultured on OP9-DL1 stroma. These data confirm the findings above that,
165 at least by the canonical markers, CD27 and CD28, ACY1215 treatment promotes differentiation
166 towards DN3b at the expense of DN3a.

167 Given that the primary function of this checkpoint is to ensure appropriate TCRβ rearrangement, we
168 assessed the correlation of each marker with TCRβ expression (**Figure 2B**). As previously shown
169 (Williams et al., 2005), expression of CD28 was clearly correlated with expression of icTCRβ in cells
170 derived from fetal liver or from the adult thymus. The $CD28^{Hi}$ cells also expressed more of the
171 nutrient transporters, CD71 and CD98, and more surface TCRβ (**Supp Fig 7A**) indicating that, in
172 general, they had progressed further through β-selection, but the correlation was not absolute. For
173 both cell sources, ACY1215 treatment resulted in less icTCRβ expression in the DN3b (whether
174 measured as $CD28^{Hi}$ or $CD27^{Hi}$ DN3 cells) (Fig 2B, see also Supp Fig 8C). To validate the icTCRβ
175 staining, we directly compared it with surface TCRβ (**Supp Fig 7B**). For both cell sources, expression
176 of surface TCRβ was highly correlated with that of icTCRβ and both were reduced by ACY1215
177 treatment. Thus, as well as depleting DN3a cells, treatment with ACY1215 increases the proportions
178 of a cell population that bears many of the phenotypic markers of passage through β-selection, but
179 these cells appear somewhat defective in expression of TCRβ, and do not progress optimally through
180 the DP stage. We speculated that further characterisation of these cells might yield valuable
181 information about requirements at the β-selection checkpoint.

182 **CD2 expression identifies $DN3b^{Pre}$ and $DN3b^{Post}$ as two functionally distinct stages in β-selection.**

183 A well-established co-stimulator of TCR signalling is CD2 (Skånland et al., 2014). Expression of
184 CD2 marks TCRβ V(D)J rearrangement and can facilitate pre-TCR signalling for passage through the
185 β-selection checkpoint (Groettrup et al., 1992; Rodewald et al., 1993; Sasada and Reinherz, 2001). In
186 the next series of experiments, we find that CD28 and CD2 reliably define 3 sequential stages of β
187 selection in DN3 cells, which we term DN3a, $DN3b^{Pre}$, and $DN3b^{Post}$ to accommodate pre-existing
188 nomenclature (**Figure 3A**). Co-staining of DMSO-treated DN3 cells with CD28 and CD2 showed that
189 all DN3a cells ($CD28^{Lo}$) were $CD2^{Lo}$, but DN3b ($CD28^{Hi}$) cells had two clearly discernible
190 populations of $CD2^{Lo}$ ($DN3b^{Pre}$) and $CD2^{Hi}$ ($DN3b^{Post}$) (**Figure 3Bi**). ACY1215 treatment enriched for

191 the DN3b^{Pre}. Cell counts indicated that the numbers of DN3b^{Pre} cells were not substantially affected
192 by ACY1215, but DN3a and DN3b^{Post} numbers were dramatically reduced (**Supp Fig 8A**). Thus,
193 ACY1215 treatment led to an enrichment in a DN3b^{Pre} population that was low for CD2. The DN3b^{Pre}
194 population **(Fig 3Bii)** was evident in thymocytes from young adult mice, even without *in vitro* culture
195 (see Fig 4 below), and was again enriched by treatment with ACY1215.

196 To confirm that DN3b^{Pre} cells were earlier in β-selection than DN3b^{Post} cells, we assessed the
197 association of CD2 expression with proliferation as measured by CFSE dilution (**Supp Fig 8B**). Two
198 clear populations were evident, with the CD2^{Hi} (DN3b^{Post}) cells having undergone substantially more
199 proliferation than the CD2^{Lo} (DN3b^{Pre}) cells. ACY1215 treatment did not disrupt the association
200 between CD2 and proliferation. Expression of CD27 and surface TCRβ were also increased from
201 DN3a, DN3b^{Pre}, to DN3b^{Post}, with stepwise correlation which was not altered by ACY1215 despite
202 lower surface TCRβ on DN3b^{Post} cells (**Supp Fig 8C**). We then assessed icTCRβ and Ki-67 staining,
203 which should reflect the cell proliferation triggered by successful passage through the β-selection
204 checkpoint (**Figure 3C**). Indeed, consistent with previous findings that TCRβ V(D)J recombination is
205 restricted to DN cells positive for CD2 (Rodewald et al., 1993), DN3b^{Pre} cells were intermediate in
206 expression of icTCRβ and Ki67, between the levels seen on DN3a cells and DN3b^{Post} cells. The
207 correlated, stepwise increase in icTCRβ and Ki-67 was observed in cultures from both fetal liver and
208 adult thymus (Figure 3Ci & ii). This pattern was even more striking in thymocytes from adult mice,
209 where DN3a cells showed no proliferation, DN3b^{Pre} cells were heterogeneous with respect to
210 proliferation, and proliferation correlated with icTCRβ expression, and DN3b^{Post} cells were all highly
211 proliferative, with minimal impact from ACY1215 treatment. These data suggest that the dramatic
212 reduction in TCRβ expression upon ACY1215 treatment observed in Fig 2 was explained more by the
213 enrichment of DN3b^{Pre} cells, by than a direct effect on TCRβ expression. c-Myc, which mediates the
214 proliferative response to pre-TCR signalling but is not required for differentiation (Dose et al., 2006),
215 showed a similar stepwise increase with these differentiation stages (**Supp Fig 8D**). These data are all
216 compatible with an interim DN3b^{Pre} stage that reflects an early, and pivotal step in β-selection where
217 rearrangement of the TCRβ chain is translated into proliferation.

218 To formally assess whether the DN3b^{Pre} stage is a transitional stage before DN3b^{Post}, we sorted DN3a,
219 DN3b^{Pre} and DN3b^{Post} cells from adult mice and cultured them for further analysis (**Figure 4**).
220 Analysis of the cells immediately after extraction (top right contour plots) showed clearly distinct
221 DN3a, DN3b^{Pre} and DN3b^{Post} cells. After two days, DN3b^{Post} cells had produced substantial numbers
222 of DP cells, with fewer produced by DN3b^{Pre}, and fewer still by DN3a cells. Also compatible with
223 unidirectional progression from DN3a to DN3b^{Pre} to DN3b^{Post}, was the proportion of DN4 and DN3
224 stages from each sorted population. ACY1215 treatment of thymocytes stabilized the DN3b^{Pre}
225 population and blocked progression to DP. Similar data was obtained in the fetal liver-derived
226 cultures (**Supp Fig 9**). These data confirm that DN3b^{Pre} (CD28^{Lo}CD2^{Lo}) is a transitional state between
227 DN3a (CD28^{Hi}CD2^{Lo}) and DN3b^{Post} (CD28^{Hi}CD2^{Hi}), reflecting partial progression through β-
228 selection.

229 **ACY1215 alters the pre-TCR signalling platform clustered at MTOC**

230 The enrichment of CD28^{Hi}CD2^{Lo} (DN3b^{Pre}) cells by ACY1215 treatment in both fetal liver-derived
231 cells and thymocytes from adult mice suggests that a key process in this stage might involve
232 acetylation. We explored three possible mechanisms by which ACY1215 might disrupt β-selection.
233 ACY1215 is selective for HDAC6, and can inhibit the catalytic activity of HDAC6 (Eich et al., 2018;
234 Narita et al., 2019). HDAC6 protein is expressed at every stage of T cell development (**Supp Fig**
235 **10A**). The best-known role of HDAC6 is in modification of histones for epigenetic regulation. Indeed,
236 acetylation of H3K18 was increased upon treatment with ACY1215, suggesting that epigenetic
237 modification could be affected by the drug (**Supp Fig 10B**). Although best known as a regulator of
238 histone acetylation, HDAC6 can also acetylate α-tubulin (Narita et al., 2019). In mature T cells, the
239 regulation of acetylation of α-tubulin by HDAC6 influences TCR-mediated recruitment of the
240 microtubule-organising centre (MTOC) to the immunological synapse (Serrador et al., 2004). In all T
241 cell developmental stages, HDAC6 was predominantly in the nucleus, but also detectable in the
242 cytoplasm and near the MTOC, compatible with effects on MTOC modification (**Supp Fig 10C-E**).
243 Acetylation of α-tubulin (K40), which can be de-acetylated by HDAC6 (Osseni et al., 2020), was
244 evident throughout the T cell differentiation stages (**Figure 5A**). Upon a two-hour treatment with

245 ACY1215, each population showed an increase in acetylated tubulin, suggesting HDAC6 deacetylated
246 tubulin throughout early T cell development.

247 We previously found that T cells undergoing β-selection form an immunological synapse, in which
248 MTOC and other TCR-associated signalling proteins move with the MTOC to the site of antigen
249 receptor signalling receptor signalling (Allam et al., 2021). We therefore speculated that an alteration
250 in MTOC organisation might mediate the effects of ACY1215 on β-selection by impacting the
251 immunological synapse. To address this, we first assessed the association of LAT with the MTOC
252 (**Figure 5B**). DN3a cells were cultured for 1 day with and without ACY1215 (so would be
253 predominantly DN3a and DN3b^{Pre} and not yet past β-selection; see Supp Fig 9). Acetyl-α-tubulin
254 presented as a single cluster in the site of the MTOC, and was increased in intensity with ACY1215
255 treatment, compatible with the flow cytometry results. LAT was strongly associated with the MTOC
256 in DMSO treated cells, but altered by ACY1215 treatment, with less intense fluorescence and less
257 clustering at the MTOC. Notch is particularly important during β-selection in mediating assembly of
258 the immunological synapse and transmitting signals downstream of the pre-TCR signal (Allam et al.,
259 2021; Charnley et al., 2020). We therefore assessed the co-localisation of Notch1 and the MTOC in
260 DN3a cells cultured for 1 day with and without ACY1215 (**Figure 5C**). In DMSO treated cells, Notch
261 was concentrated at the MTOC, but, similar to LAT, was much more diffuse following ACY1215
262 treatment. Interestingly, the change in localisation of both Notch and LAT was accompanied by a loss
263 in their intensity. A reduction in surface Notch expression was observed in DN3a, DN3b and DN4
264 cells, suggesting that the reduction in Notch1 transcription that normally occurs following β-selection
265 (Yashiro-Ohtani et al., 2009) might be accelerated by ACY1215 (**Figure 5D**). Together, these data
266 suggest that a possible mechanistic basis for the effects of ACY1215 on β-selection is via alterations
267 in recruitment by MTOC of Notch1 and TCR signalling components to the immunological synapse,
268 associated with enhanced tubulin acetylation at the immunological synapse.

269 **DN3b^{Pre} cells have commenced but not completed β-selection, and are controlled by sequential**
270 **changes in key regulators of β-selection.**

271 How might such a disruption in the immunological synapse and TCR signalling alter progression
272 from DN3b^{Pre} to DN3b^{Post}? A collaboration between pre-TCR and Wnt signalling is well established,
273 with two core Wnt pathway transcriptional regulators: β-catenin and Lef1/TCF-1 essential to β-
274 selection (Gounari et al., 2001; López-Rodríguez et al., 2015; Staal and Clevers, 2005; Travis et al.,
275 1991; Xu et al., 2009; Zhao et al., 2021). TCF-1 and Lef1 can directly modify histone acetylation, and
276 this function is inhibited by the pharmacological HDAC inhibitors, Tubacin and Vorinostat, (Xing et
277 al., 2016; Zhao et al., 2021). In support of functional interplay between ACY1215 treatment and TCF-
278 1 and Lef1, TCF-1 deficiency leads to a similar phenotype as ACY1215 treatment, with disrupted β-
279 selection and reduced expression of icTCRβ in DN4 cells (Goux et al., 2005), and deletion of both
280 TCF-1 and Lef1 leads to a complete block at DN4 (Yu et al., 2012). We focused on Lef1 since Lef1 is
281 specifically expressed at the β-selection stage (Mingueneau et al., 2013). To assess whether Lef1
282 might mediate the β-selection decisions at the DN3b^{Pre} stage, we explored how its expression changed
283 with differentiation, and how it was impacted by ACY1215 treatment. Lef1 was minimally expressed
284 in DN3a cells, uniformly bright in DN3b^{Post} cells, but heterogeneous in DN3b^{Pre} cells derived from
285 either fetal liver or adult thymus (**Figure 6Ai & ii**). In the DN3b^{Pre} cells, Lef1-expression was
286 associated with increased expression of TCRβ, albeit with a wide range in TCRβ expression (**Figure**
287 **6B**). ACY1215 treatment did not demonstrably alter icTCRβ expression (Figure 6B) but, prevented
288 the upregulation of Lef1 expression in DN3b^{Pre} cells, suggesting a role in pre-TCR-mediated
289 induction of Lef1.

290 The correlation in expression of TCRβ with proliferation and Lef1 expression raised the possibility
291 that the pre-TCR signal might be directly translated into phenotype during the DN3b^{Pre} stage. To
292 explore this, we investigated the TCR-associated receptor, CD5. A role for CD5 has not been
293 demonstrated during β-selection, but during positive selection expression of CD5 reports the strength
294 of TCR signalling and tunes TCR signalling responsiveness, dampening the response of cells to TCR-
295 signalling via the NF-κB pathway (Azzam et al., 2001; Azzam et al., 1998; Tarakhovsky et al., 1995;
296 Voisinne et al., 2018). To explore the dynamics of CD5 expression during β-selection, we stained
297 fetal liver-derived DN3 cells with CD2, Lef1 and CD5 (**Supp Fig 11**). Gating for DN3b^{Pre} with low

298 and high Lef1 expression showed strong correlation of CD5 and Lef1expression. Interestingly, Lef1
299 upregulation was retained in the presence of ACY1215, but the correlation with CD5 expression was
300 lost. These data suggest a model in which CD5 expression is downstream of Lef1, and suggest the
301 effects of ACY1215 on progression through β-selection might be mediated by disrupting the
302 functional connection between Lef1 and CD5. Lef1 and CD5 expression were similarly correlated in
303 DN3 cells extracted from the adult thymus, particularly in DN3b^{Pre} cells (**Figure 7A**).

304 To confirm this model, we made use of the fact that progression past DN3 is marked by
305 downregulation of CD25, and a transitional stage between DN3b and DN4 (sometimes termed DN3c)
306 can be identified within the DN3 population (Ananias et al., 2008; Teague et al., 2010). We therefore
307 assessed the relationship between CD2 and CD25 in the DN3b cells. DN3b^{Pre} population was still
308 high for CD25, but DN3b^{post} included CD25^{Lo} cells (**Supp Fig 12A**). These data are compatible with
309 the notion that DN3b^{Post} marks a later stage in differentiation, that includes, but is not exclusive to, the
310 DN3c population (Ananias et al., 2008). To assess whether the combined expression of CD5 and Lef1
311 in DN3b cells indicated progression through β-selection, we gated for the two clearly discriminated
312 sub-populations Lef1^{Lo}CD5^{Lo} and Lef1^{Hi}CD5^{Hi}, and compared their CD25 expression (**Supp Fig**
313 **12B**). The Lef1^{Hi}CD5^{Hi} cells were substantially lower for CD25, indicating that they had already
314 progressed through β-selection. Although as expected there were far fewer cells in the Lef1^{Hi}CD5^{Hi}
315 population upon ACY1215 treatment, they also exhibited the reduction in CD25, suggesting that
316 ACY1215-treated cells can precociously differentiate beyond β-selection in the absence of CD5
317 expression.

318 To confirm the relationship between pre-TCR and CD5 and to assess the impact of ACY121, we
319 cultured DN3a or DN3b cells from adult thymus in the presence of ACY1215 or DMSO for 2 days,
320 gated for DN3b cells, and compared CD5 expression to icTCRβ (**Figure 7B**). Cells from the DN3a
321 starting population were more likely to be dull for both CD5 and icTCRβ, compared with the more
322 mature cells from the DN3b starting population. However, in these mature cells, expression of
323 icTCRβ correlated with expression of CD5, suggesting that, as in other cell types, CD5 expression
324 might report TCR signalling strength during β-selection. In ACY1215-treated cells, expression of

325 surface TCRβ was reduced by the DN3b^{Post} stage, and uncoupled from CD5. Similar findings were
326 obtained using fetal liver cultures and staining for CD5 and icTCRβ (**Supp Fig 13**). The correlation of
327 TCRβ with CD5, and its uncoupling after ACY1215 treatment, was not observed with CD27 and
328 CD28 (Figure 2) nor CD2 (Figure 3). Together, a functional link between pre-TCR, Lef1and CD5 is
329 coordinated at DN3b^{Pre} stage (**Figure 7C**), and is affected by ACY1215.

330 To assess the functional relationship between TCRβ and CD5, we compared CD5 expression and
331 proliferation in the presence and absence of ACY1215 (**Figure 8A**). Proliferation was minimal in
332 most DN3a cells and DN3b^{Pre} cells, but was evident in a portion of DN3b^{Pre}, cells from the DN3b
333 starting population, and in DN3b^{Post} cells. This proliferation was clearly correlated with CD5
334 expression in control cells. However, the correlation between CD5 expression and CFSE dilution was
335 lost in the DN3b^{Pre} cells that had been treated with ACY1215. These data together indicate that CD5
336 is functionally connected to both TCRβ expression and proliferation, and that this functional
337 association is broken by ACY1215 treatment.

338

339 **Discussion**

340 A critical factor in β-selection is the sequential expression of specific transcriptional regulators, with
341 differential perdurance and cross-inhibition ensuring checks and balances that prevent inappropriate
342 survival and differentiation (Chann and Russell, 2019; Zhao et al., 2021). Many such checks and
343 balances have been identified to play important roles during β-selection, but the stepwise progression
344 of events that dictate fate have been elusive (Chann and Russell, 2019; Zhao et al., 2021). Our
345 explorations into effects of an HDAC6 inhibitor have revealed sa new working model (**Figure 8B,**
346 **Supp Fig 14**), Once DN3b^{Pre} cells have entered the β-selection checkpoint, they respond to graded
347 levels of TCRβ by expressing Lef1, then CD5. Normally, proliferation only occurs in cells expressing
348 CD5. Passing of the β-selection checkpoint is then marked by the expression of CD2. The disruption
349 in TCRβ-associated expression of CD5 by ACY1215 provides a possible mechanism for the escape of

350 cells lacking an appropriately rearranged TCRβ chain following ACY1215 treatment, although such a
351 role remains to be investigated.

352 The upregulation of CD27 and CD28 is gradual, but the upregulation of CD2 is more abrupt, making
353 for a convenient demarcation of differentiation stages. Our findings are compatible with previous
354 observations that CD2 expression marks cells with TCRβ gene rearrangement (Rodewald et al.,
355 1993), that knockout of CD2 inhibits progression to the DN4 stage but does not influence TCRβ
356 repertoire (Sasada and Reinherz, 2001), and suggestions of cis-regulation of CD2 and TCRβ
357 expression involving chromatin structure (Kamoun et al., 1995) Together, these findings suggest that
358 expression of CD2 (marking entrance to the DN3b^{Post} stage) reflects a completion of TCRβ
359 recombination and triggers critical fate-determining events that involve progressive upregulation of
360 CD5 and Lef1. CD2 in mature T cells sets quantitative thresholds for activation (Bachmann et al.,
361 1999), suggesting the possibility that a similar process could be involved in β-selection.

362 **Ideas and Speculation**

363 A novel finding from this work is that CD5 levels are modified in association with pre-TCR
364 expression, and that treatment with ACY1215 prevents the upregulation of CD5 (but has a lesser
365 effect on Lef1 upregulation) during β-selection. At other stages of T cell development and activation,
366 CD5 reports on the strength of TCR signalling, with increasing expression reflecting a stronger TCR
367 signal (Azzam et al., 1998; Sood et al., 2021; Tarakhovsky et al., 1995). Our findings that the
368 correlation of CD5 with TCRβ expression is lost with ACY1215 treatment, but the correlation of CD5
369 expression with proliferation is retained with ACY1215 treatment, suggest the possibility that CD5
370 plays a similar role as a reporter of pre-TCR signalling. Interestingly, it is now emerging that
371 differential CD5 expression also marks the propensity for different fates in thymocytes and CD4^{+} T
372 cells, and this reflects transcriptional and epigenetic differences between cells with high and low CD5
373 expression (Rogers et al., 2021). In other cell types the combined action of responding to, and
374 dampening, the TCR signal, allows CD5 to tune the TCR signal and so shift the window and modify
375 the timing of positive selection (Lutes et al., 2021; Matson et al., 2020; Sood et al., 2021; Voisinne et
376 al., 2018). Whether or not such a tuning role might occur for CD5 during β-selection needs further

377 exploration, but a possible role for tuning of the TCRβ repertoire during β selection is made relevant
378 by findings that the pre-TCR can bind with low affinity to MHC-peptide (Li et al., 2021; Mallis et al.,
379 2015). The pre-TCR also forms an immunological synapse with many similarities to the
380 immunological synapse formed by the αβTCR, oriented towards MHC (Allam et al., 2021). More
381 work is needed to determine any functional connection between CD5 and tuning, or epigenetic
382 modifications during β-selection, but these data point to a role for CD5 during the DN3b^{Pre} stage in
383 reporting pre-TCR activity to determine subsequent passage through the β-selection checkpoint.

384 The molecular basis by which ACY1215 mediates the effects on cell fate we observe here needs
385 more exploration. There are many possible means by which ACY1215 might impact upon
386 transcriptional and epigenetic alterations during β-selection to mediate the phonotypes we observe
387 here. At β-selection, transient activation of β-catenin mediates TCF-1 and Lef1 transcriptional
388 regulation to promote pre-TCR-dependent transition to the DN4 stage (Xu et al., 2009). Ectopic
389 expression of a constitutively active β-catenin allows the cells to bypass pre-TCR signalling, yielding
390 DN4 cells lacking expression of TCRβ (Gounari et al., 2001). The similarities between this phenotype
391 and the apparent bypass of pre-TCR signalling we observe with ACY1215 treatment suggest TCF-
392 1/Lef might mediate the effects of ACY1215. Indeed, HDAC6 can regulate acetylation of β-catenin to
393 coordinate its degradation, providing a possible mechanism for the effects of ACY1215 on TCF-1/Lef
394 activity (Iaconelli et al., 2015). Given the correlation between Lef1 expression and CD5 we observe,
395 CD5 might be downstream of Lef1 during β-selection, perhaps explaining the ACY1215-mediated
396 deregulation of CD5 expression. These findings suggest that the induction of Lef1 at the DN3b^{Pre}
397 stage is coordinated with pre-TCR signalling, in part to promote CD5 expression, and that this activity
398 can be altered by ACY1215 treatment. Whether the effect of ACY1215 relates to HDAC6, an
399 alternative HDAC, or the histone deacetylase activity of Lef1/TCF-1 remains to be determined.

400 Other molecular mediators downstream of ACY1215 effects are also possible. It was recently shown
401 that the transcriptional repressor, Bcl6, is induced by pre-TCR signalling and required for passage
402 through the β-selection checkpoint (Solanki et al., 2020). Differentiation of T follicular helper cells
403 also requires Bcl6, in this case induced by Lef1 and TCF (Choi et al., 2015). Several HDACs have

404 been shown to complex with and modulate Bcl6 activity to impact on B cell development and
405 function (Wang et al., 2020). Together with our findings, these studies suggest the possibility that
406 ACY1215 might mediate at least some of its effects via Bcl6. HDAC6 has also been implicated in the
407 DNA damage response (Zhang et al., 2019), raising the possibility that ACY1215 effects might relate
408 to the genetic recombination integral to the creation of a TCRβ chain (Miyazaki et al., 2008). In any
409 case, the functional outcome of ACY1215 treatment is to disrupt the connections between pre-TCR
410 signalling and expression of CD5 expression and CD5-associated proliferation. Uncoupling CD5 from
411 TCRβ and Lef1 expression provides a possible mechanism by which ACY1215 allows the wrong
412 cells (perhaps cells without suitable TCRβ) to proliferate and differentiate to DN3b^{Post} cells, but these
413 cells subsequently fail to progress, leading to the block in DP differentiation.

414 The known role for HDAC6 in linking tubulin acetylation to the immunological synapse of mature T
415 cells (Serrador et al., 2004), and our finding that acetylation of α-tubulin is increased in DN3 cells,
416 suggested the possibility that the β-selection immunological synapse might mediate the effects of
417 ACY125. Indeed, ACY1215 does alter the organisation of the TCR signalling molecules, LAT,
418 around the MTOC. Similarly, Notch1, which is required to enhance the polarisation of the pre-TCR
419 (Allam et al., 2021; Charnley et al., 2020), is lost from the MTOC following ACY1215 treatment.
420 These findings are particularly interesting in light of a recent report that HDAC6 is required for the
421 formation of aggresomes at the MTOC (Magupalli et al., 2020), and suggest that HDAC6 might play
422 a more general role in coordinating recruitment to the MTOC. An alternative explanation for the
423 effect of ACY1215 on β-selection relates to observations that HDAC inhibitors can induce MHC
424 constituents to promote antigen presentation (Magner et al., 2000). It remains to be determined
425 whether an influence on stromal-presented peptide-MHC plays any role in disrupting β-selection.
426 Interestingly, both CD2 and CD5 can regulate activity of the immunological synapse and connectivity
427 to the MTOC (Brossard et al., 2003; Dustin et al., 1998; Tibaldi et al., 2002) further supporting the
428 possibility that the immunological synapse provides a hub at which deacetylation and pre-TCR
429 signalling converge. Together, these findings suggest that the effect of HDAC6 on β-selection that we
430 see here might occur through disruption of the DN3 immunological synapse.

431 The molecular basis for the effects of ACY1215 on β-selection might therefore by multifaceted, and
432 relate to one or more of direct alteration of the epigenome to influence protein expression, alteration
433 of Lef1 activity, DNA damage response, alteration of pre-TCR signalling via organisation at the
434 MTOC and the immunological synapse. Irrespective of the molecular mechanism, the finding that
435 AY1215 disrupts T cell development has potential implications for the development of clinical
436 applications of small molecule inhibitors of HDAC6, particularly in treatment of young patients,
437 whose T cell repertoire has not yet been established (Cosenza and Pozzi, 2018; Hogg et al., 2020).

438

439 **Materials and Methods**

440 ***Ex vivo* culture of developing T cells and drug treatments**

441 Two sources to derive developing T cells were employed in this study: mouse hematopoietic stem
442 cells (HSCs) and mouse primary thymocytes. HSCs were collected from C57BL/6 mouse E14.5
443 fetal liver. To induce *ex vivo* T cell development, HSCs were co-cultured with OP9-DL1 stromal
444 cells (from Juan Carlos Zúñiga-Pflücker, University of Toronto, Toronto, Canada) at a 1:1 ratio in a
445 6-well plate (2×10^5). The coculture was maintained in αMEM (Sigma-Aldrich, M4526),
446 supplemented with foetal calf serum (10% v/v), glutamine (1 mM), β-mercaptoethanol (50 μM),
447 sodium pyruvate (1nM), HEPES (10 mM), penicillin/streptomycin (100 ng/mL), mouse interleukin 7
448 (1 ng/mL) and mouse FMS-like tyrosine kinase 3 (5 ng/ml). C57BL/6 mice at 4-5 week were
449 euthanised for thymus collection. The primary thymocytes were released from thymus for sorting,
450 analysis or further culturing with OP9-DL1 stromal cells under the same culture conditions as the
451 HSC system described above. For both sources of developing T cells, ACY1215, purchased from
452 MedChemExpress (NJ, USA), was used at 1 μM as described (Laino et al., 2019). ACY1215 was
453 dissolved in DMSO to 5 mM, and diluted to 1 μM with culture media immediately prior to application
454 to cells. The small-molecule inhibitor of Stat5, Pimozide (CAS 2062-78-4 Sigma-Aldrich) was used
455 at a final concentration of 10 μM. The selective inhibitor of p300 and CBP, C646 (Sigma-Aldrich)
456 was used at 2.5 μM. OP9-DL1 stromal cells was maintained in αMEM (Sigma-Aldrich, M4526)

457 supplemented with 20% (v/v) fetal calf serum, glutamine (1 mM) and penicillin/streptomycin (100
458 ng/mL). When OP9-DL1 stromal cells were confluent after 3-4 days of coculture, primary thymocytes
459 were dissociated from the stromal cells through forceful pipetting, and were harvested with the fresh
460 OP9-DL1 stromal cells.

461 **Flow Cytometry and western blot**

462 To purify T cell populations using flow cytometry, primary thymocytes were dissociated from OP9-
463 DL1 stromal cell, and were resuspended in PBS buffer containing 2% FBS and antibody cocktail for
464 surface staining. Antibody cocktails were comprised of lineage markers (NK-1.1, CD11b, CD45R,
465 Ly6G6C, Ter119), and differentiation markers (CD4, CD8, CD25, CD44, CD28 and CD2; details
466 about fluorochrome, manufacturer and dilution are summarised in the supplementary materials).
467 Primary thymocytes were incubated with antibody cocktails for 40 minutes before FACS.

468 Flow cytometry (BD Aria III) was used to analyse and sort the populations of developing T cells.
469 DN3 cells were identified based on surface expression (Lineage^{-}, CD4^{-}, CD8^{-}, CD25^{Hi}, CD44^{Lo}).
470 DN3a cells were DN3 cell with CD28^{L0}, by contrast, DN3b cells were DN3 cell with CD28^{Hi}. DP
471 cells were identified based on surface expression (Lineage^{-}, CD4^{+}, CD8^{+}).

472 To detect intracellular expression of TCRβ, Ki67, Lef1, c-Myc, Notch1, HDAC6 and H3K18ac, the
473 Foxp3/Transcription Factor Staining Buffer Kit (eBioscience) was used according to the
474 manufacturer's instruction. Briefly, the primary thymocytes after surface staining were incubated with
475 fixative for 15 minutes in dark, room temperature, followed with centrifuge and washing out the
476 fixative. To detect expression of acetyl-tubulin, the cells were fixed with IC Fixation Buffer
477 (eBioscience) for 15 minutes in dark, room temperature, followed with centrifuge and washing out the
478 fixative. The fixed cells were then incubated with antibody for flow cytometry analysis.

479 To detect tubulin acetylation by western blotting, cells were lysed in RIPA buffer , and lysates were
480 subjected to SDS-PAGE and probed with antibodies to tubulin and acetylated tubulin.

481

482 **Immunofluorescence staining and confocal microscopy**

483 The sorted DN3a or DN3b were grown on glass-bottomed 8-well chambers (ibidi) with OP9-DL1
484 stromal cells, and were fixed with 4% formaldehyde for 8 minutes at room temperature followed by
485 0.1% Triton X-100 permeabilization for 5 minutes. The samples were then incubated with primary
486 antibody overnight at 4°C (details about antibody usage is summarised in Supplementary table 1).
487 After the primary antibody being washed out by PBS, the cells were labelled with fluorochrome-
488 conjugated secondary antibodies (as Table S1), DAPI (Thermo Fisher Scientific), and Phalloidin
489 (Abcam). The samples were examined using a FV3000 confocal microscope (Olympus) and 60X lens
490 (1.30 NA, UPLSAPO, Olympus). The images were processed with maximum intensity projection
491 using Image J. The mean intensity of region of interest was examined in Image J.

492 **Data collection and Statistical analyses**

493 Python (version 3.8.1) was used to visualise the statistics. Data of flow cytometry were analysed by
494 FlowJo software (version X10.0.7r2. Tree Star, Inc.). The bar plot was shown as mean ± SEM. More
495 than three repeats were included in the statistics and were colour-coded for each individual repeat.
496 Microsoft Excel (version 2016) was used for two sided t-test, by which p value was indicated.

497

Acknowledgements

This work was done on Wurundjeri land of the Kulin nation, and we pay our respects to the Elders past and present. We thank Louise Cheng, Callum Dark, Amr Allam and Peter Fraser for technical assistance and helpful discussions, and Ellis Reinherz, Jonathon Duke-Cohan for helpful comments on the manuscript. The work was funded by Australian Research Council (FT0990405 to SMR), National Health and Medical Research Council (APP1099140 to SMR), Swinburne University Postgraduate Research Award to ASC.

Competing Interest Statement

No author declares any competing interests

Author Contribution Statement

Conceptualization: ASC, SMR
Methodology: ASC, MC, SMR
Experimentation: ASC, FW
Visualization: ASC, SMR
Supervision: POH, RWJ, SMR, TT
Writing—original draft: ASC, SMR
Writing—review & editing: ASC, MC, LN, AN, POH, RWJ, SMR

Ethics

C57bl/6 mouse E14.5 fetal livers and 4-5-week mouse thymi were collected according to Peter MacCallum Cancer Centre Ethics Committee approval E627 and La Trobe University Animal Ethics Committee approval AEC-20024.

526 ## Figure Legends

527 **Figure 1. ACY1215 inhibits T cell development at the DN3 stage**

528 **(A)** FL-derived developing T cells were treated with ACY1215 or DMSO for 2 days as indicated, and
529 the Lin^- cells were assessed for CD4 and CD8 expression to determine the proportions of DN and
530 DPpopulations. The DN (Lin^-, $CD4^-$, $CD8^-$) cells were assessed for CD44 and CD25 expression to
531 determine the proportions of DN3 and DN4 populations. The frequency of each population was
532 summarised in a swarm plot, with individual colours representing each experiment.

533 Sorted, FL-derived DN3a cells **(B)** or thymocytes **(C)** were cultured under ACY1215 or DMSO
534 treatment for 1 or 2 days as indicated, and the $CD44^-$ DN population (representing DN3 and DN4
535 stages) was assessed for CD25 and CD28 expression. The frequency of each population were
536 summarised in swarm plots, with individual colours representing each experiment. Cell numbers were
537 summarised in line plots.

538 **(D)** Sorted, FL-derived DN3b cells were cultured for 4 days under ACY1215 or DMSO treatment as
539 indicated, and cell numbers per population were estimated by multiplying the total cell number by the
540 frequency and were summarised in the line chart.

541

542 **Figure 2. ACY1215 inhibits β-selection.**

543 **(A)** Developing T cells from FL **(i)** or the adult thymus **(ii)** were treated with ACY1215 or DMSO for
544 1 day or 2 days, and the DN3 cells were assessed for CD27 and CD28 expression to discriminate
545 DN3a and DN3b. Cell number or frequency were summarised in the swarm plot, with individual
546 colours representing each experiment.

547 **(B)** Sorted, FL-derived DN3a cells **(i)** were cultured under ACY1215 or DMSO treatment for 4 days
548 as indicated, and DN3 cells were assessed for the expressions of intracellular TCRβ (icTCRβ) versus
549 CD28 or CD27. Thymocytes **(ii)** were cultured under ACY1215 or DMSO treatment for 1 day as

550 indicated, and DN3 cells were assessed for the expressions of icTCRβ versus CD28. The frequency of
551 icTCRβ^{+} cells was summarised in a swarm plot, with individual colours representing each experiment.

552

553 **Figure 3. CD2 upregulation discriminates DN3b^{Pre} and DN3b^{Post} populations**

554 **(A)** The strategy for discriminating between three populations (DN3a, DN3b^{Pre}, and DN3b^{Post}) is
555 indicated in the schematic.

556 **(B)** FL-derived developing T cells **(i)** or the sorted thymocyte DN3 **(ii)** were treated with ACY1215
557 or DMSO for 1 or 2 days, and the DN3 cells were assessed for CD2 and CD28 expression.

558 **(C)** FL-derived developing T cells **(i)** or the sorted thymus-derived DN3 **(ii)** were treated with
559 ACY1215 or DMSO for 1 day, and DN3a, DN3b^{Pre}, and DN3b^{Post} cells were assessed for icTCRβ and
560 Ki-67 expression. MFI of icTCRβ and Ki-67 were summarised in histogram and swarm plot, with
561 individual colours representing each experiment. (p value < 0.001 = '***', < 0.01 = '**', <0.05 ='*')

562

563 **Figure 4. DN3a, DN3b^{Pre} and DN3b^{Post} stages follow a sequential progression.**

564 The DN3a, DN3b^{Pre}, and DN3b^{Post} cells from the adult thymus were sorted as indicated, and were
565 cultured on OP9-DL1. At two day, the cells were analysed by CD4 versus CD8, the DN cells were
566 analysed by CD44 versus CD25, and the DN3 cells were analysed by CD2 versus CD28. The
567 frequencies of each population were summarised in the line plots. (p value < 0.001 = '***', < 0.01 =
568 '**', <0.05 ='*')

569

570 **Figure 5. ACY1215 alters pre-TCR signalling clustered at the MTOC.**

571 **(A)** Sorted FL-derived DN, DP, CD4-SP, CD8-SP, DN1, DN2, DN3a, DN3b were treated with
572 ACY1215 or DMSO for 2 hours as indicated, and were assessed for acetyl-α-tubulin (K40) as shown

573 in histograms. The white histogram are unstained controls in which cells from each sorting were
574 stained with secondary antibody only.

575 **(B, C)** Sorted FL-derived DN3a cells were treated with ACY1215 or DMSO for 1 day as indicated,
576 followed by immunostaining for LAT, acetyl-α-tubulin (K40), Notch1 and α-tubulin. The mean
577 intensity of acetyl-α-tubulin, LAT and the ratio of Notch1 expressed at MTOC versus at nucleus were
578 summarized in violin plot overlaid with box plot. Cell number for LAT staining: ACY1215 (n=55)
579 and DMSO (n=54); Cell number for acetyl-α-tubulin (K40) staining: ACY1215 (n=30) and DMSO
580 (n=31); Cell number for Notch1 staining: ACY1215 (n=56) and DMSO (n=55).

581 **(D)** FL-derived developing T cells were treated with ACY1215 or DMSO for 2 day, and the DN3a,
582 DN3b and DN4 cells were assessed for Notch1 expression, as summarised in swarm plot, with
583 individual colours representing each experiment.

584

585 **Figure 6. Coordinated upregulation of Lef1 and TCRβ in DN3b^{Pre} cells.**

586 **(A)** FL-derived developing T cells **(i)** or the sorted thymocyte DN3 **(ii)** were treated with ACY1215 or
587 DMSO for 1 day as indicated, and DN3 cells were assessed for CD2 and CD28 expression. The
588 DN3a, DN3b^{Pre}, and DN3b^{Post} cells were assessed for Lef1 expression.

589 **(B)** DN3a, DN3b^{Pre}, and DN3b^{Post} cells from (A, i) were assessed for Lef1 and icTCRβ expression.

590

591 **Figure 7. CD5 is upregulated with Lef1 and TCRβ in DN3b^{Post} cells.**

592 **(A)** Sorted DN3 cells from the adult thymus were treated with ACY1215 or DMSO for 1 day as
593 indicated, and DN3 cells were assessed for CD5, CD2 and Lef1 expression.

594 **(B)** Sorted DN3a and DN3b^{Pre} cells from the adult thymus were treated with ACY1215 or DMSO for
595 2 day as indicated, and DN3 populations were assessed for CD5 and surface TCRβ expression.

596 (C) Schematic describes the stepwise expression of TCR co-receptors (CD28, CD5, and CD2) and
597 Lef1 from DN3a, DN3b^{Pre} to DN3b^{Post} stage.

598

599 **Figure 8. CD5 upregulation correlates with the passing of β-selection checkpoint**

600 **(A)** Sorted FL-derived DN3a and DN3b were stained with CFSE after sorting and were cultured with
601 ACY1215 or DMSO for two days as indicated. At two days, the DN3a, DN3b^{Pre}, and DN3b^{Post} cells
602 from the sorted DN3a and DN3b were assessed for CD5 expression versus CFSE intensity.

603 **(B)** Schematic summarises the working model of molecular interactions at the DN3b^{Pre} stage. Firstly,
604 CD28 (the defining step in transition from DN3a to DN3b^{Pre}) acts to promote signalling through the
605 nascent pre-TCR. Second, pre-TCR signals induce expression of CD5 (or *vice versa*) and lead to the
606 passing of the β-selection checkpoint. By coordinating transcriptional control, functional MTOC and
607 immunological synapse formation for survival, proliferation and differentiation. Possible molecular
608 events disrupted by ACY1215 treatment to cause these cellular responses are indicated by the red
609 double lines.

610

611 **Figure S1.**

612 **(A)** A schematic of the stages of T cell development and the cell surface markers used to differentiate
613 them. Cells were classed as DN (Double Negative, lacking expression of CD4 and CD8), and
614 progressed from DN1 to DN4 according to their expression of CD44 and CD25 as indicated. β-
615 selection occurs at the DN3 stage, as cells progress from DN3a to DN3b, indicated by upregulation of
616 CD28. Cells post β-selection progressed from DN4 to the DP stage (Double Positive, expressing both
617 CD4 and CD8) before committing to SP (Single Positive for either CD4 or CD8).

618 **(B)** Fetal liver cells were collected from E14.5 mice embryos, and cells cultured on OP9-D1L stromal
619 cells for 8-10 days. The developing T cells were demarcated as the flow indicated.

620 **(C)** Thymocytes were collected from 4-to-5-week mice thymus **(i)** and/or were cultured *ex vivo* on
621 OP9-DL1 stromal cells **(ii)**. The developing T cells were demarcated as the flow indicated.

622

623 **Figure S2.**

624 OP9-DL1 were plated at a density of twenty thousand cells per well, and were cultured with
625 ACY1215 (1μM) LMK235 (0.5μM) or control DMSO (1 in 1000 dilution) for two days. (A) Cell
626 numbers were counted as shown in the bar chart.

627 (B) OP9-DL1 treated with DMSO and ACY1215 for 2 days were assessed for the protein level of
628 acetyl-α-tubulin (K40) and α-tubulin. In a parallel experiment, drug was replaced with fresh media
629 and thymocytes were added for coculture. The media was changed every hour. After three hours,
630 thymocytes attached on the OP9-DL1 were counted as shown in the bar chart.

631 (C) OP9-DL1 cells pre-treated with DMSO and ACY1215 were cultured with sorted thymic DN3 for
632 0.5 day. Thymocytes were re-plated twice further on to fresh OP9-DL1 that had been pre-treated with
633 DMSO and ACY1215 as indicated in the flow chart. After 1.5 day, thymocyte differentiation was
634 assessed by CD4 and CD8 expression.

635 (D) Sorted, FL-derived DN2, DN3a, DN3b and DP were cultured for 2 days with ACY1215 or
636 DMSO treatment as indicated. Cell numbers were counted at 3 hours and 2 days, and the proliferation
637 rate (2 days / 3 hours) was summarised in swarm plot, with individual colours representing
638 independent experiments.

639

640 **Figure S3.**

641 **(A)** Sorted, FL-derived DN3a and DN3b were stained with CFSE after sorting and were cultured with
642 ACY1215 or DMSO for two days as indicated. At one hour post sorting, the intensity of CFSE were
643 recorded, as indicated by the white histogram. At two days, the DN3 cells from the sorted DN3a and

644 DN3b were assessed for CD28 expression and CFSE intensity, as shown in the contour plots and the
645 histograms.

646 **(B)** FL-derived developing T cells were treated with ACY1215 or DMSO for 1 day as indicated, and
647 DN3a and DN3b cells were assessed for FSC and Ki-67 expression.

648

649 **Figure S4.**

650 **(A)** Sorted, FL-derived DN3a, DN3b and DP cells were treated with ACY1215 or DMSO for 3 hours
651 or 6 hours as indicated, followed with propidium iodide (PI) staining to label dead cells. The
652 frequency of PI^+ population were summarised in swarm plot, with individual colours representing
653 each experiment.

654 **(B)** Sorted, FL-derived DN3a and DN3b cells were treated with ACY1215 or DMSO for 6 hours or 1
655 day with or without OP9-DL1 coculture as indicated. The cells were assessed for Annexin V
656 expression and DAPI intensity as shown in the density plot.

657

658 **Figure S5.**

659 Sorted, FL-derived DN3a **(A)** and sorted, FL-derived DN3b **(B)** were cultured for 4 days under
660 ACY1215 or DMSO treatment as indicated, and were analysed by CD4 and CD8 **(i)** and CD44 and
661 CD25 **(ii)**. The frequency of each population was summarised in swarm plot, with individual colours
662 representing independent experiments.

663

664 **Figure S6.**

665 **(A)** FL-derived developing T cells were treated with ACY1215 or DMSO for 2 days as indicated, and
666 DN3a, DN3b, DN4 and DP cells were assessed for surface TCRβ and surface TCRγδ expression. **(B)**
667 Sorted, FL-derived DN3b cells were cultured for 2 days under ACY1215 or DMSO treatment as

668 indicated, and DN3, DN4 and DP cells were assessed for surface TCRβ and surface TCRγδ
669 expression. **(C)** Sorted FL-derived DN3b cells were cultured for 4 days under ACY1215 or DMSO
670 treatment as indicated, and DN3, DN4 and DP cells were assessed for intracellular TCRβ (icTCRβ)
671 and CD28 expression. The frequency and cell number were summarised in swarm plot, with
672 individual colours representing each experiment.

673

674 **Figure S7.**

675 **(A)** CD28 upregulation marks both DN3 cells differentiation and passing β-selection. FL-derived
676 developing T cells at around day 8-10 of coculture with OP9-DL1 stromal cells were assessed for
677 CD28, CD71, CD98, CD27 and surface TCRβ expression.

678 **(B)** Sorted, FL-derived DN3b **(i)** or thymocytes **(ii)** were treated with ACY1215 or DMSO for 1 day
679 or 2 days as indicated, and the DN3 cells were assessed for surface TCRβ and icTCRβ expression.
680 MFI of surface TCRβ from icTCRβ^{+} cells was summarised in a swarm plot, with individual colours
681 representing each experiment.

682

683 **Figure S8**

684 **(A)** Quantification for Figure 3A. Frequency and cell number of the three populations (DN3a,
685 DN3b^{Pre}, and DN3b^{Post}) was summarised in swarm plots, with individual colours representing each
686 experiment.

687 **(B)** Sorted, FL-derived DN3a and DN3b were stained with CFSE after sorting and were cultured with
688 ACY1215 or DMSO for two days as indicated. At two days, the DN3 cells from the sorted DN3a and
689 DN3b were assessed for CD2 expression versus CFSE intensity.

690 **(C)** DN3a, DN3b^{Pre}, and DN3b^{Post} thymocytes that treated with ACY1215 for 1 day were assessed for
691 CD27 and surface TCRβ expression.

692 **(D)** FL-derived developing T cells were treated with ACY1215 or DMSO for 2 days, and DN3a,
693 DN3b^{Pre}, and DN3b^{Post} cells were assessed for c-Myc expression.

694

695 **Figure S9**

696 FL-derived developing T cells were treated with DMSO or ACY1215 for 1.5 day, and DN3a,
697 DN3b^{Pre}, and DN3b^{Post} cells were sorted as indicated **(i)**. At one day, the cells were analysed by CD4
698 versus CD8 **(ii)** and CD2 versus CD28 **(iii)**. The frequencies of each population were summarised in
699 the line plots. (p value < 0.001 = '***', < 0.01 = '**', <0.05 ='*')

700

701 **Figure S10.**

702 HDAC6 is expressed in developing T cells. **(A)** To examine HDAC6 protein expression, FL-derived
703 developing T cells treated with DMSO or ACY1215 for two days were fixed by cytoplasmic fixative
704 or nuclear fixative, followed by examination of HDAC6 expression. **(B)** FL-derived developing T
705 cells were treated with ACY1215, the selective inhibitor of p300 and CBP, C646, or DMSO for 1 day
706 as indicated, and the expression of H3K18ac were assessed and shown in the histogram. **(C)** Sorted,
707 FL-derived DN3a or DN3b cells were assessed for HDAC6 (in white colour) expression by
708 immunostaining. **(D, E)** Sorted, FL-derived DN3b cells were treated with ACY1215 or DMSO for 1
709 day, followed by immunostaining for α-tubulin, Arp2 (in white colour), acetyl-α-tubulin (K40) (in
710 white colour).

711

712 **Figure S11.**

713 FL-derived developing T cells were treated with ACY1215 or DMSO for 1 day as indicated **(i)**, and
714 DN3a, DN3b^{Pre}, and DN3b^{Post} cells were assessed for Lef1, CD2 and CD5 expression. DN3b^{Pre} cells
715 were further characterised by Lef1^{Hi} or Lef1^{Lo}, and were assessed for Lef1 and CD5 expression with

716 DN3a and DN3b^{Post}. Expression of Lef1 and CD5 at the DN3a, DN3b^{Pre}, and DN3b^{Post} stage was
717 quantified at (i) and (ii).

718

719 **Figure S12.**

720 **(A)** Sorted FL-derived DN3b^{Pre} cells were accessed for CD25 expression as schematic indicated.

721 **(B)** FL-derived developing T cells were treated with ACY1215 or DMSO for 2 days as indicated, and
722 DN3a and DN3b were assessed for Lef1 and CD5 expression. The expression of CD25 in the DN3b
723 subsets and DN4 were shown in histogram.

724 **Figure S13.**

725 Sorted FL-derived DN3a and DN3b cells were treated with DMSO or ACY1215 for 2 days, and were
726 assessed for CD5, TCRβ and CD25 expression.

727

728 **Figure S14.**

729 Schematic shows the sequence of protein expression changes during development from DN3a,
730 DN3b^{Pre} to DN3b^{Post}.

731

732 **References**

733 Adeegbe, D.O., Y. Liu, P.H. Lizotte, Y. Kamihara, A.R. Aref, C. Almonte, R. Dries, Y. Li, S. Liu, X. Wang,
734 T. Warner-Hatten, J. Castrillon, G.C. Yuan, N. Poudel-Neupane, H. Zhang, J.L. Guerriero, S.
735 Han, M.M. Awad, D.A. Barbie, J. Ritz, S.S. Jones, P.S. Hammerman, J. Bradner, S.N. Quayle,
736 and K.K. Wong. 2017. Synergistic Immunostimulatory Effects and Therapeutic Benefit of
737 Combined Histone Deacetylase and Bromodomain Inhibition in Non-Small Cell Lung Cancer.
738 *Cancer discovery* 7:852-867.
739 Allam, A.H., M. Charnley, K. Pham, and S.M. Russell. 2021. Developing T cells form an immunological
740 synapse for passage through the beta-selection checkpoint. *J Cell Biol* 220:
741 Ananias, H.J., I.J. de Jong, R.A. Dierckx, C. van de Wiele, W. Helfrich, and P.H. Elsinga. 2008. Nuclear
742 imaging of prostate cancer with gastrin-releasing-peptide-receptor targeted
743 radiopharmaceuticals. *Current pharmaceutical design* 14:3033-3047.
744 Azzam, H.S., J.B. DeJarnette, K. Huang, R. Emmons, C.-S. Park, C.L. Sommers, D. El-Khoury, E.W.
745 Shores, and P.E. Love. 2001. Fine Tuning of TCR Signaling by CD5. *The Journal of Immunology*
746 166:5464-5472.
747 Azzam, H.S., A. Grinberg, K. Lui, H. Shen, E.W. Shores, and P.E. Love. 1998. CD5 expression is
748 developmentally regulated by T cell receptor (TCR) signals and TCR avidity. *J Exp Med*
749 188:2301-2311.
750 Bachmann, M.F., M. Barner, and M. Kopf. 1999. CD2 sets quantitative thresholds in T cell activation.
751 *J Exp Med* 190:1383-1392.
752 Ballesteros-Arias, L., J.G. Silva, R.A. Paiva, B. Carbonetto, P. Faisca, and V.C. Martins. 2019. T Cell
753 Acute Lymphoblastic Leukemia as a Consequence of Thymus Autonomy. *J Immunol*
754 Brossard, C., M. Semichon, A. Trautmann, and G. Bismuth. 2003. CD5 inhibits signaling at the
755 immunological synapse without impairing its formation. *J Immunol* 170:4623-4629.
756 Chann, A.S., and S.M. Russell. 2019. An integrated transcriptional switch at the beta-selection
757 checkpoint determines T cell survival, development and leukaemogenesis. *Biochemical*
758 *Society transactions* 47:1077-1089.
759 Charnley, M., M. Ludford-Menting, K. Pham, and S.M. Russell. 2020. A new role for Notch in the
760 control of polarity and asymmetric cell division of developing T cells. *J Cell Sci* 133:jcs235358.
761 Choi, Y.S., J.A. Gullicksrud, S. Xing, Z. Zeng, Q. Shan, F. Li, P.E. Love, W. Peng, H.H. Xue, and S. Crotty.
762 2015. LEF-1 and TCF-1 orchestrate T differentiation by regulating differentiation circuits
763 upstream of the transcriptional repressor Bcl6. *Nat Immunol*
764 Cosenza, M., and S. Pozzi. 2018. The Therapeutic Strategy of HDAC6 Inhibitors in
765 Lymphoproliferative Disease. *International journal of molecular sciences* 19:
766 Dose, M., I. Khan, Z. Guo, D. Kovalovsky, A. Krueger, H. von Boehmer, K. Khazaie, and F. Gounari.
767 2006. c-Myc mediates pre-TCR-induced proliferation but not developmental progression.
768 *Blood* 108:2669-2677.
769 Douek, D.C., R.A. Vescio, M.R. Betts, J.M. Brenchley, B.J. Hill, L. Zhang, J.R. Berenson, R.H. Collins,
770 and R.A. Koup. 2000. Assessment of thymic output in adults after haematopoietic stem-cell
771 transplantation and prediction of T-cell reconstitution. *Lancet* 355:1875-1881.
772 Dustin, M.L., M.W. Olszowy, A.D. Holdorf, J. Li, S. Bromley, N. Desai, P. Widder, F. Rosenberger, P.A.
773 van der Merwe, P.M. Allen, and A.S. Shaw. 1998. A novel adaptor protein orchestrates
774 receptor patterning and cytoskeletal polarity in T-cell contacts. *Cell* 94:667-677.
775 Dutta, A., B. Zhao, and P.E. Love. 2021. New insights into TCR β-selection. *Trends in Immunology*
776 Eich, C., J. Arlt, C.S. Vink, P. Solaimani Kartalaei, P. Kaimakis, S.A. Mariani, R. van der Linden, W.A. van
777 Cappellen, and E. Dzierzak. 2018. In vivo single cell analysis reveals Gata2 dynamics in cells
778 transitioning to hematopoietic fate. *The Journal of Experimental Medicine* 215:233-248.
779 Gounari, F., I. Aifantis, K. Khazaie, S. Hoeflinger, N. Harada, M.M. Taketo, and H. von Boehmer. 2001.
780 Somatic activation of beta-catenin bypasses pre-TCR signaling and TCR selection in
781 thymocyte development. *Nat Immunol* 2:863-869.

782 Goux, D., J.D. Coudert, D. Maurice, L. Scarpellino, G. Jeannet, S. Piccolo, K. Weston, J. Huelsken, and
783 W. Held. 2005. Cooperating pre-T-cell receptor and TCF-1-dependent signals ensure
784 thymocyte survival. *Blood* 106:1726-1733.
785 Groettrup, M., A. Baron, G. Griffiths, R. Palacios, and H. von Boehmer. 1992. T cell receptor (TCR)
786 beta chain homodimers on the surface of immature but not mature alpha, gamma, delta
787 chain deficient T cell lines. *EMBO J* 11:2735-2745.
788 Hayday, A.C., and D.J. Pennington. 2007. Key factors in the organized chaos of early T cell
789 development. *Nat Immunol* 8:137-144.
790 Hogg, S.J., P.A. Beavis, M.A. Dawson, and R.W. Johnstone. 2020. Targeting the epigenetic regulation
791 of antitumour immunity. *Nature reviews. Drug discovery*
792 Holmes, R., and J.C. Zúñiga-Pflücker. 2009. The OP9-DL1 system: generation of T-lymphocytes from
793 embryonic or hematopoietic stem cells in vitro. *Cold Spring Harb Protoc* 2009:pdb.prot5156.
794 Iaconelli, J., J.H. Huang, S.S. Berkovitch, S. Chattopadhyay, R. Mazitschek, S.L. Schreiber, S.J.
795 Haggarty, and R. Karmacharya. 2015. HDAC6 inhibitors modulate Lys49 acetylation and
796 membrane localization of beta-catenin in human iPSC-derived neuronal cells. *ACS Chem Biol*
797 10:883-890.
798 Kamoun, M., J.S. Woods, N. Sano, H. Makni, R. Smith, W.B. de Lau, A. van Oers, D. Wotton, M.J.
799 Owen, Y. Hashimoto, and H.C. Clevers. 1995. Analysis of CD2 and TCR-beta gene expression
800 in Jurkat cell mutants suggests a cis regulation of gene transcription. *J Immunol* 155:3929-
801 3937.
802 Laino, A.S., B.C. Betts, A. Veerapathran, I. Dolgalev, A. Sarnaik, S.N. Quayle, S.S. Jones, J.S. Weber,
803 and D.M. Woods. 2019. HDAC6 selective inhibition of melanoma patient T-cells augments
804 anti-tumor characteristics. *Journal for immunotherapy of cancer* 7:33.
805 Li, X., R. Mizsei, K. Tan, R.J. Mallis, J.S. Duke-Cohan, A. Akitsu, P.W. Tetteh, A. Dubey, W. Hwang, G.
806 Wagner, M.J. Lang, H. Arthanari, J.H. Wang, and E.L. Reinherz. 2021. Pre-T cell receptors
807 topologically sample self-ligands during thymocyte beta-selection. *Science* 371:181-185.
808 López-Rodríguez, C., J. Aramburu, and R. Berga-Bolaños. 2015. Transcription factors and target genes
809 of pre-TCR signaling. *Cellular and Molecular Life Sciences* 72:2305-2321.
810 Lutes, L.K., Z. Steier, L.L. McIntyre, S. Pandey, J. Kaminski, A.R. Hoover, S. Ariotti, A. Streets, N. Yosef,
811 and E.A. Robey. 2021. T cell self-reactivity during thymic development dictates the timing of
812 positive selection. *eLife* 10:e65435.
813 Magner, W.J., A.L. Kazim, C. Stewart, M.A. Romano, G. Catalano, C. Grande, N. Keiser, F. Santaniello,
814 and T.B. Tomasi. 2000. Activation of MHC class I, II, and CD40 gene expression by histone
815 deacetylase inhibitors. *J Immunol* 165:7017-7024.
816 Magupalli, V.G., R. Negro, Y. Tian, A.V. Hauenstein, G. Di Caprio, W. Skillern, Q. Deng, P. Orning, H.B.
817 Alam, Z. Maliga, H. Sharif, J.J. Hu, C.L. Evavold, J.C. Kagan, F.I. Schmidt, K.A. Fitzgerald, T.
818 Kirchhausen, Y. Li, and H. Wu. 2020. HDAC6 mediates an aggresome-like mechanism for
819 NLRP3 and pyrin inflammasome activation. *Science* 369:eaas8995.
820 Mallis, R.J., K. Bai, H. Arthanari, R.E. Hussey, M. Handley, Z. Li, L. Chingozha, J.S. Duke-Cohan, H. Lu,
821 J.H. Wang, C. Zhu, G. Wagner, and E.L. Reinherz. 2015. Pre-TCR ligand binding impacts
822 thymocyte development before alphabetaTCR expression. *Proc Natl Acad Sci U S A*
823 112:8373-8378.
824 Matson, C.A., S. Choi, F. Livak, B. Zhao, A. Mitra, P.E. Love, and N.J. Singh. 2020. CD5 dynamically
825 calibrates basal NF-kappaB signaling in T cells during thymic development and peripheral
826 activation. *Proc Natl Acad Sci U S A* 117:14342-14353.
827 Mingueneau, M., T. Kreslavsky, D. Gray, T. Heng, R. Cruse, J. Ericson, S. Bendall, M.H. Spitzer, G.P.
828 Nolan, K. Kobayashi, H. von Boehmer, D. Mathis, C. Benoist, C. Immunological Genome, A.J.
829 Best, J. Knell, A. Goldrath, V. Jojic, D. Koller, T. Shay, A. Regev, N. Cohen, P. Brennan, M.
830 Brenner, F. Kim, T.N. Rao, A. Wagers, T. Heng, J. Ericson, K. Rothamel, A. Ortiz-Lopez, D.
831 Mathis, C. Benoist, N.A. Bezman, J.C. Sun, G. Min-Oo, C.C. Kim, L.L. Lanier, J. Miller, B. Brown,
832 M. Merad, E.L. Gautier, C. Jakubzick, G.J. Randolph, P. Monach, D.A. Blair, M.L. Dustin, S.A.

833 Shinton, R.R. Hardy, D. Laidlaw, J. Collins, R. Gazit, D.J. Rossi, N. Malhotra, K. Sylvia, J. Kang,
834 T. Kreslavsky, A. Fletcher, K. Elpek, A. Bellemare-Pelletier, D. Malhotra, and S. Turley. 2013.
835 The transcriptional landscape of alphabeta T cell differentiation. *Nat Immunol* 14:619-632.
836 Miyazaki, M., K. Miyazaki, M. Itoi, Y. Katoh, Y. Guo, R. Kanno, Y. Katoh-Fukui, H. Honda, T. Amagai,
837 M. van Lohuizen, H. Kawamoto, and M. Kanno. 2008. Thymocyte proliferation induced by
838 pre-T cell receptor signaling is maintained through polycomb gene product Bmi-1-mediated
839 Cdkn2a repression. *Immunity* 28:231-245.
840 Narita, T., B.T. Weinert, and C. Choudhary. 2019. Functions and mechanisms of non-histone protein
841 acetylation. *Nature Reviews Molecular Cell Biology* 20:156-174.
842 Notarangelo, L.D., R. Bacchetta, J.L. Casanova, and H.C. Su. 2020. Human inborn errors of immunity:
843 An expanding universe. *Science Immunology* 5:eabb1662.
844 Osseni, A., A. Ravel-Chapuis, J.-L. Thomas, V. Gache, L. Schaeffer, and B.J. Jasmin. 2020. HDAC6
845 regulates microtubule stability and clustering of AChRs at neuromuscular junctions. *Journal*
846 *of Cell Biology* 219:
847 Rodewald, H.R., K. Awad, P. Moingeon, L. D'Adamio, D. Rabinowitz, Y. Shinkai, F.W. Alt, and E.L.
848 Reinherz. 1993. Fc gamma RII/III and CD2 expression mark distinct subpopulations of
849 immature CD4-CD8- murine thymocytes: in vivo developmental kinetics and T cell receptor
850 beta chain rearrangement status. *J Exp Med* 177:1079-1092.
851 Rogers, D., A. Sood, H. Wang, J.J.P. van Beek, T.J. Rademaker, P. Artusa, C. Schneider, C. Shen, D.C.
852 Wong, M.-È. Lebel, S.A. Condotta, M.J. Richer, A.J. Martins, J.S. Tsang, L. Barreiro, P.
853 Francois, D. Langlais, H.J. Melichar, J. Textor, and J.N. Mandl. 2021. Pre-existing chromatin
854 accessibility and gene expression differences among naïve CD4⁺ T cells
855 influence effector potential. *bioRxiv* 2021.2004.2021.440846.
856 Sasada, T., and E.L. Reinherz. 2001. A critical role for CD2 in both thymic selection events and mature
857 T cell function. *J Immunol* 166:2394-2403.
858 Serrador, J.M., J.R. Cabrero, D. Sancho, M. Mittelbrunn, A. Urzainqui, and F. Sanchez-Madrid. 2004.
859 HDAC6 deacetylase activity links the tubulin cytoskeleton with immune synapse
860 organization. *Immunity* 20:417-428.
861 Shapiro, M.J., and V.S. Shapiro. 2020. Chromatin-Modifying Enzymes in T Cell Development. *Annu*
862 *Rev Immunol* 38:397-419.
863 Skånland, Sigrid S., K. Moltu, T. Berge, Einar M. Aandahl, and K. Taskén. 2014. T-cell co-stimulation
864 through the CD2 and CD28 co-receptors induces distinct signalling responses. *Biochemical*
865 *Journal* 460:399-410.
866 Solanki, A., D.C. Yánez, C.-I. Lau, J. Rowell, A. Barbarulo, S. Ross, H. Sahni, and T. Crompton. 2020.
867 The transcriptional repressor Bcl6 promotes pre-TCR-induced thymocyte differentiation and
868 attenuates Notch1 activation. *Development* 147:dev192203.
869 Sood, A., M.E. Lebel, M. Dong, M. Fournier, S.J. Vobecky, E. Haddad, J.S. Delisle, J.N. Mandl, N.
870 Vrisekoop, and H.J. Melichar. 2021. CD5 levels define functionally heterogeneous
871 populations of naive human CD4(+) T cells. *Eur J Immunol* 51:1365-1376.
872 Staal, F.J., and H.C. Clevers. 2005. WNT signalling and haematopoiesis: a WNT-WNT situation. *Nat*
873 *Rev Immunol* 5:21-30.
874 Taghon, T., M.A. Yui, R. Pant, R.A. Diamond, and E.V. Rothenberg. 2006. Developmental and
875 molecular characterization of emerging beta- and gammadelta-selected pre-T cells in the
876 adult mouse thymus. *Immunity* 24:53-64.
877 Tarakhovsky, A., S.B. Kanner, J. Hombach, J.A. Ledbetter, W. Muller, N. Killeen, and K. Rajewsky.
878 1995. A role for CD5 in TCR-mediated signal transduction and thymocyte selection. *Science*
879 269:535-537.
880 Teague, T.K., C. Tan, J.H. Marino, B.K. Davis, A.A. Taylor, R.W. Huey, and C.J. Van De Wiele. 2010.
881 CD28 expression redefines thymocyte development during the pre-T to DP transition. *Int*
882 *Immunol* 22:387-397.

883 Tibaldi, E.V., R. Salgia, and E.L. Reinherz. 2002. CD2 molecules redistribute to the uropod during T
884 cell scanning: implications for cellular activation and immune surveillance. *Proc Natl Acad Sci*
885 *U S A* 99:7582-7587.
886 Travis, A., A. Amsterdam, C. Belanger, and R. Grosschedl. 1991. LEF-1, a gene encoding a lymphoid-
887 specific protein with an HMG domain, regulates T-cell receptor alpha enhancer function
888 [corrected]. *Genes Dev* 5:880-894.
889 Tsuji, G., N. Okiyama, V.A. Villarroel, and S.I. Katz. 2015. Histone deacetylase 6 inhibition impairs
890 effector CD8 T-cell functions during skin inflammation. *J Allergy Clin Immunol* 135:1228-
891 1239.
892 Voisinne, G., A. Gonzalez de Peredo, and R. Roncagalli. 2018. CD5, an Undercover Regulator of TCR
893 Signaling. *Frontiers in Immunology* 9:
894 Wang, P., Z. Wang, and J. Liu. 2020. Role of HDACs in normal and malignant hematopoiesis.
895 *Molecular cancer* 19:5.
896 Williams, J.A., K.S. Hathcock, D. Klug, Y. Harada, B. Choudhury, J.P. Allison, R. Abe, and R.J. Hodes.
897 2005. Regulated costimulation in the thymus is critical for T cell development: dysregulated
898 CD28 costimulation can bypass the pre-TCR checkpoint. *J Immunol* 175:4199-4207.
899 Xing, S., F. Li, Z. Zeng, Y. Zhao, S. Yu, Q. Shan, Y. Li, F.C. Phillips, P.K. Maina, H.H. Qi, C. Liu, J. Zhu,
900 R.M. Pope, C.A. Musselman, C. Zeng, W. Peng, and H.H. Xue. 2016. Tcf1 and Lef1
901 transcription factors establish CD8 T cell identity through intrinsic HDAC activity. *Nat*
902 *Immunol*
903 Xu, K., W.Y. Yang, G.K. Nanayakkara, Y. Shao, F. Yang, W. Hu, E.T. Choi, H. Wang, and X. Yang. 2018.
904 GATA3, HDAC6, and BCL6 Regulate FOXP3+ Treg Plasticity and Determine Treg Conversion
905 into Either Novel Antigen-Presenting Cell-Like Treg or Th1-Treg. *Frontiers in immunology*
906 9:45.
907 Xu, M., A. Sharma, D.L. Wiest, and J.M. Sen. 2009. Pre-TCR-induced beta-catenin facilitates traversal
908 through beta-selection. *J Immunol* 182:751-758.
909 Yashiro-Ohtani, Y., Y. He, T. Ohtani, M.E. Jones, O. Shestova, L. Xu, T.C. Fang, M.Y. Chiang, A.M.
910 Intlekofer, S.C. Blacklow, Y. Zhuang, and W.S. Pear. 2009. Pre-TCR signaling inactivates
911 Notch1 transcription by antagonizing E2A. *Genes Dev* 23:1665-1676.
912 Yu, S., X. Zhou, F.C. Steinke, C. Liu, S.C. Chen, O. Zagorodna, X. Jing, Y. Yokota, D.K. Meyerholz, C.G.
913 Mullighan, C.M. Knudson, D.M. Zhao, and H.H. Xue. 2012. The TCF-1 and LEF-1 transcription
914 factors have cooperative and opposing roles in T cell development and malignancy.
915 *Immunity* 37:813-826.
916 Zhang, M., C. Hu, N. Moses, J. Haakenson, S. Xiang, D. Quan, B. Fang, Z. Yang, W. Bai, G. Bepler, G.M.
917 Li, and X.M. Zhang. 2019. HDAC6 regulates DNA damage response via deacetylating MLH1. *J*
918 *Biol Chem* 294:5813-5826.
919 Zhang, X.-H., M. Qin, H.-P. Wu, M.Y. Khamis, Y.-H. Li, L.-Y. Ma, and H.-M. Liu. 2021. A Review of
920 Progress in Histone Deacetylase 6 Inhibitors Research: Structural Specificity and Functional
921 Diversity. *Journal of medicinal chemistry* 64:1362-1391.
922 Zhang, Y., S. Kwon, T. Yamaguchi, F. Cubizolles, S. Rousseaux, M. Kneissel, C. Cao, N. Li, H.L. Cheng, K.
923 Chua, D. Lombard, A. Mizeracki, G. Matthias, F.W. Alt, S. Khochbin, and P. Matthias. 2008.
924 Mice lacking histone deacetylase 6 have hyperacetylated tubulin but are viable and develop
925 normally. *Mol Cell Biol* 28:1688-1701.
926 Zhao, X., Q. Shan, and H.-H. Xue. 2021. TCF1 in T cell immunity: a broadened frontier. *Nature*
927 *Reviews Immunology*

928

Figure 1.

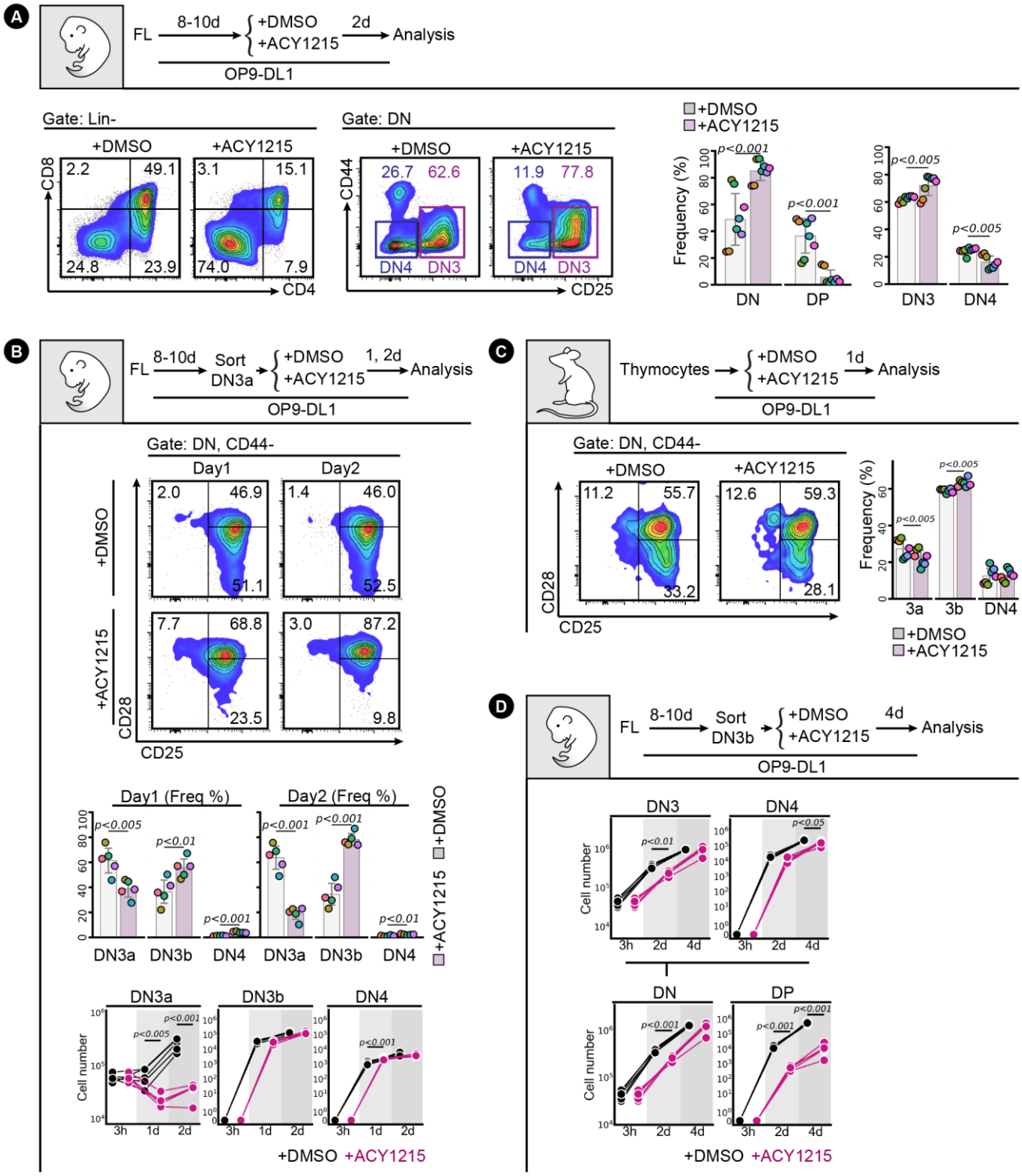
A
FL
8-10d
+DMSO
+ACY1215
2d
Analysis
OP9-DL1
Gate: Lin-
+DMSO
+ACY1215
CD8
CD4
2.2
49.1
24.8
23.9
3.1
15.1
74.0
7.9
Gate: DN
CD44
CD25
26.7
62.6
DN4
DN3
11.9
77.8
+DMSO
+ACY1215
Frequency (%)
p<0.001
p<0.005
DN
DP
DN3
DN4
B
FL
8-10d
Sort
DN3a
+DMSO
+ACY1215
1, 2d
Analysis
OP9-DL1
Gate: DN, CD44-
Day1
Day2
+DMSO
+ACY1215
CD28
CD25
2.0
46.9
51.1
1.4
46.0
52.5
7.7
68.8
23.5
3.0
87.2
9.8
Day1 (Freq %)
Day2 (Freq %)
p<0.005
p<0.01
p<0.001
DN3a
DN3b
DN4
+ACY1215
+DMSO
Cell number
3h
1d
2d
+DMSO
+ACY1215
C
Thymocytes
+DMSO
+ACY1215
1d
Analysis
OP9-DL1
Gate: DN, CD44-
+DMSO
+ACY1215
CD28
CD25
11.2
55.7
33.2
12.6
59.3
28.1
Frequency (%)
p<0.005
3a
3b
DN4
+DMSO
+ACY1215
D
FL
8-10d
Sort
DN3b
+DMSO
+ACY1215
4d
Analysis
OP9-DL1
DN3
DN4
p<0.01
p<0.05
Cell number
3h
2d
4d
DN
DP
p<0.001
+DMSO
+ACY1215

Figure 2.

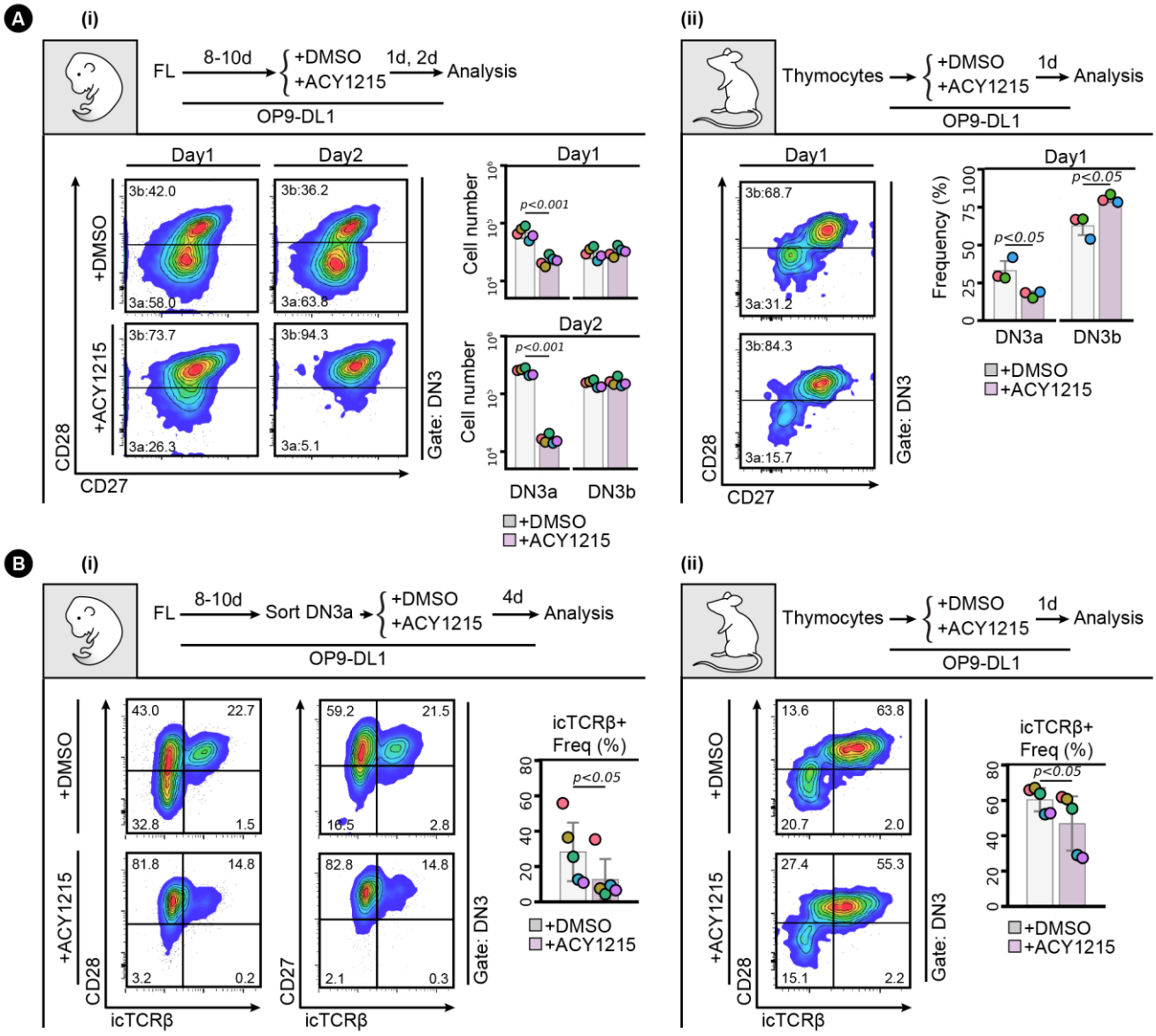
A
(i)
FL
8-10d
+DMSO
+ACY1215
1d, 2d
Analysis
OP9-DL1
Day1
Day2
3b:42.0
3a:58.0
3b:36.2
3a:63.8
3b:73.7
3a:26.3
3b:94.3
3a:5.1
+DMSO
+ACY1215
CD28
CD27
Gate: DN3
Cell number
p<0.001
DN3a
DN3b
(ii)
Thymocytes
1d
3b:68.7
3a:31.2
3b:84.3
3a:15.7
Frequency (%)
p<0.05
B
Sort DN3a
4d
43.0
22.7
32.8
1.5
81.8
14.8
3.2
0.2
59.2
21.5
16.5
2.8
82.8
14.8
2.1
0.3
icTCRβ
icTCRβ+
Freq (%)
13.6
63.8
20.7
2.0
27.4
55.3
15.1
2.2

Figure 3.

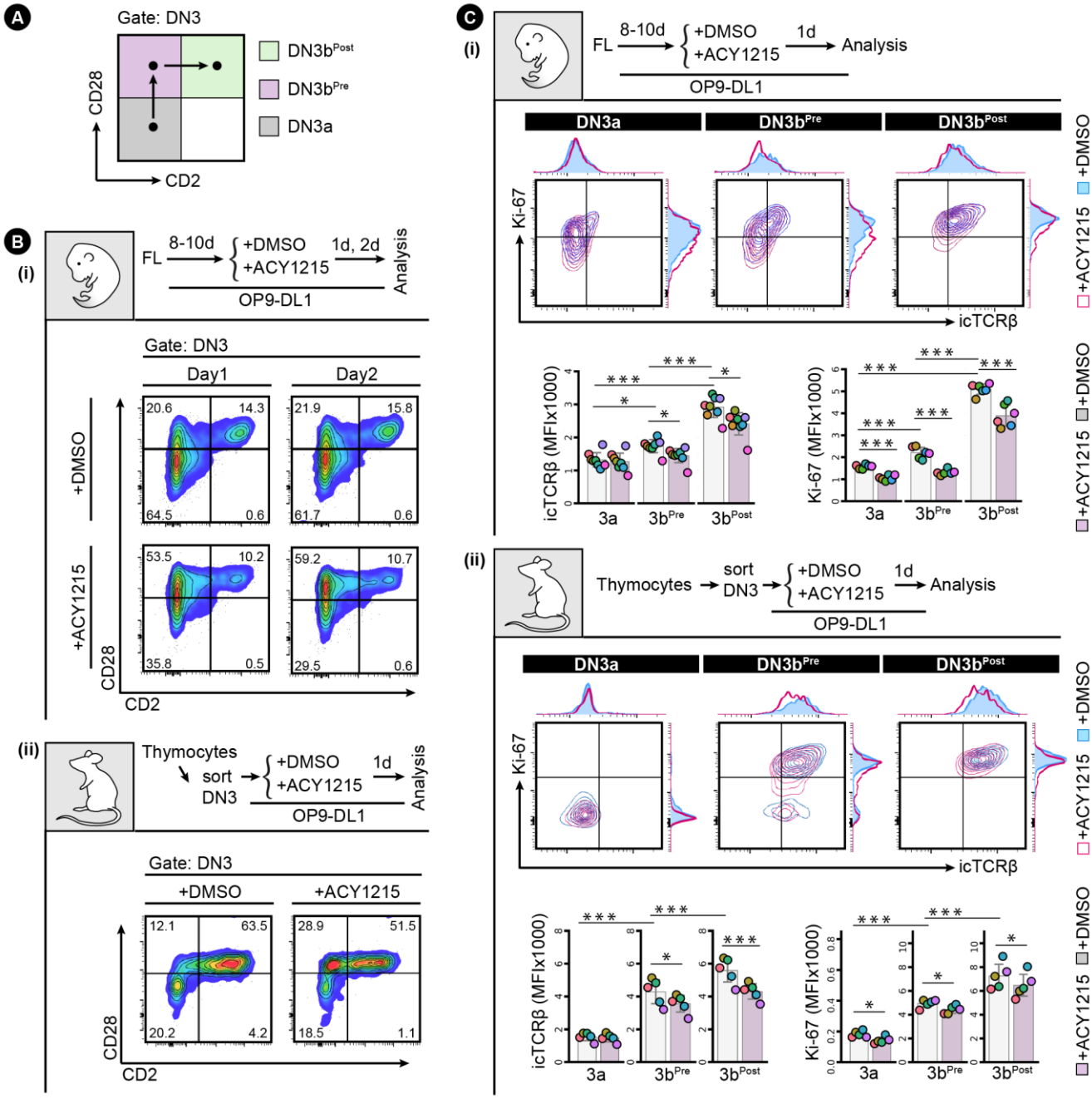

Chann et al. TCR co-receptors are expressed sequentially to fine-tune early αβ T cell development

Figure 4.

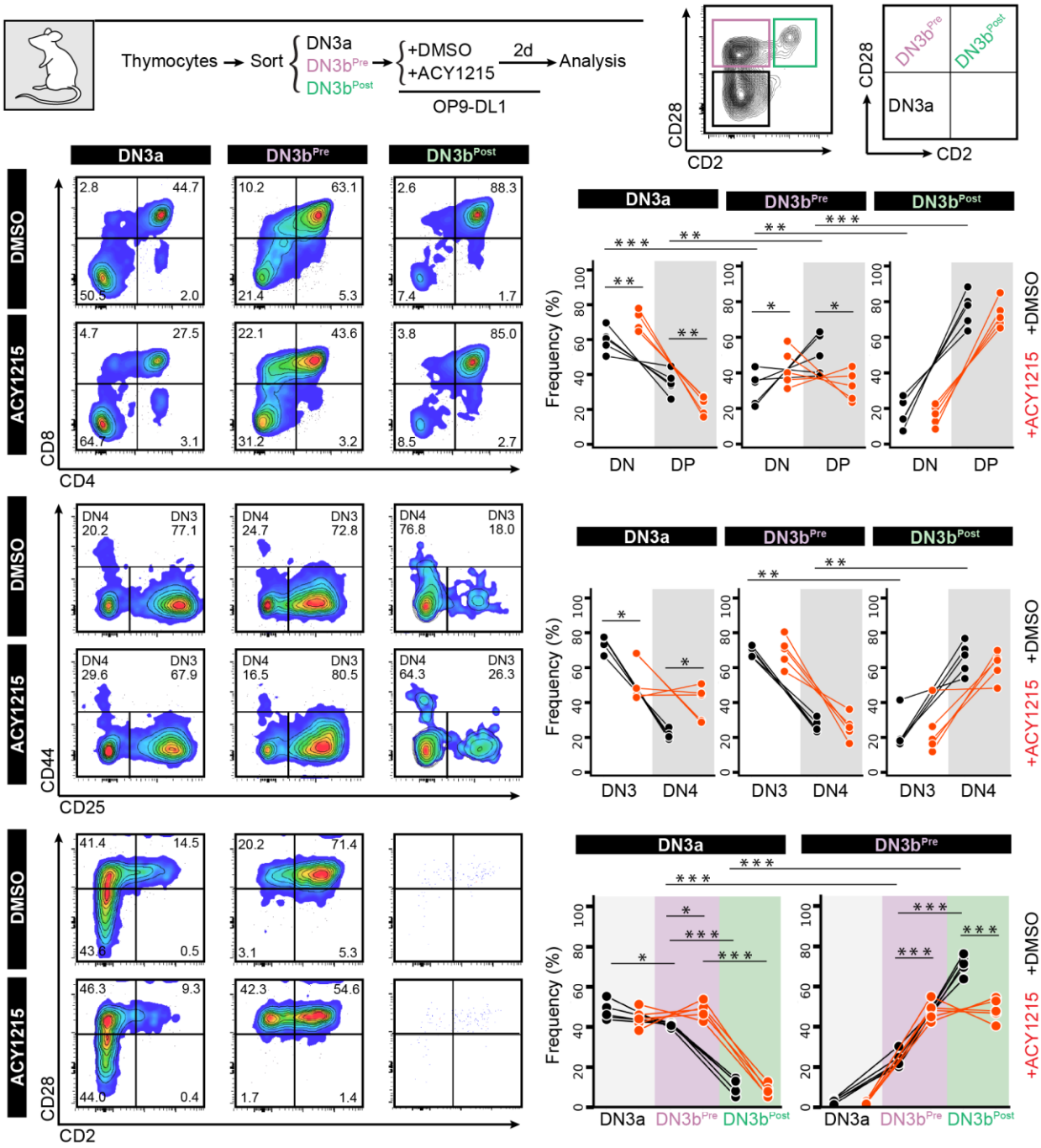
Thymocytes → Sort
DN3a
DN3b^Pre
DN3b^Post
+DMSO
+ACY1215
2d
Analysis
OP9-DL1
CD28
CD2
DN3b^Pre
DN3b^Post
DN3a
DMSO
ACY1215
CD8
CD4
CD44
CD25
Frequency (%)
DN
DP
DN3
DN4
+DMSO
+ACY1215

Figure 5.

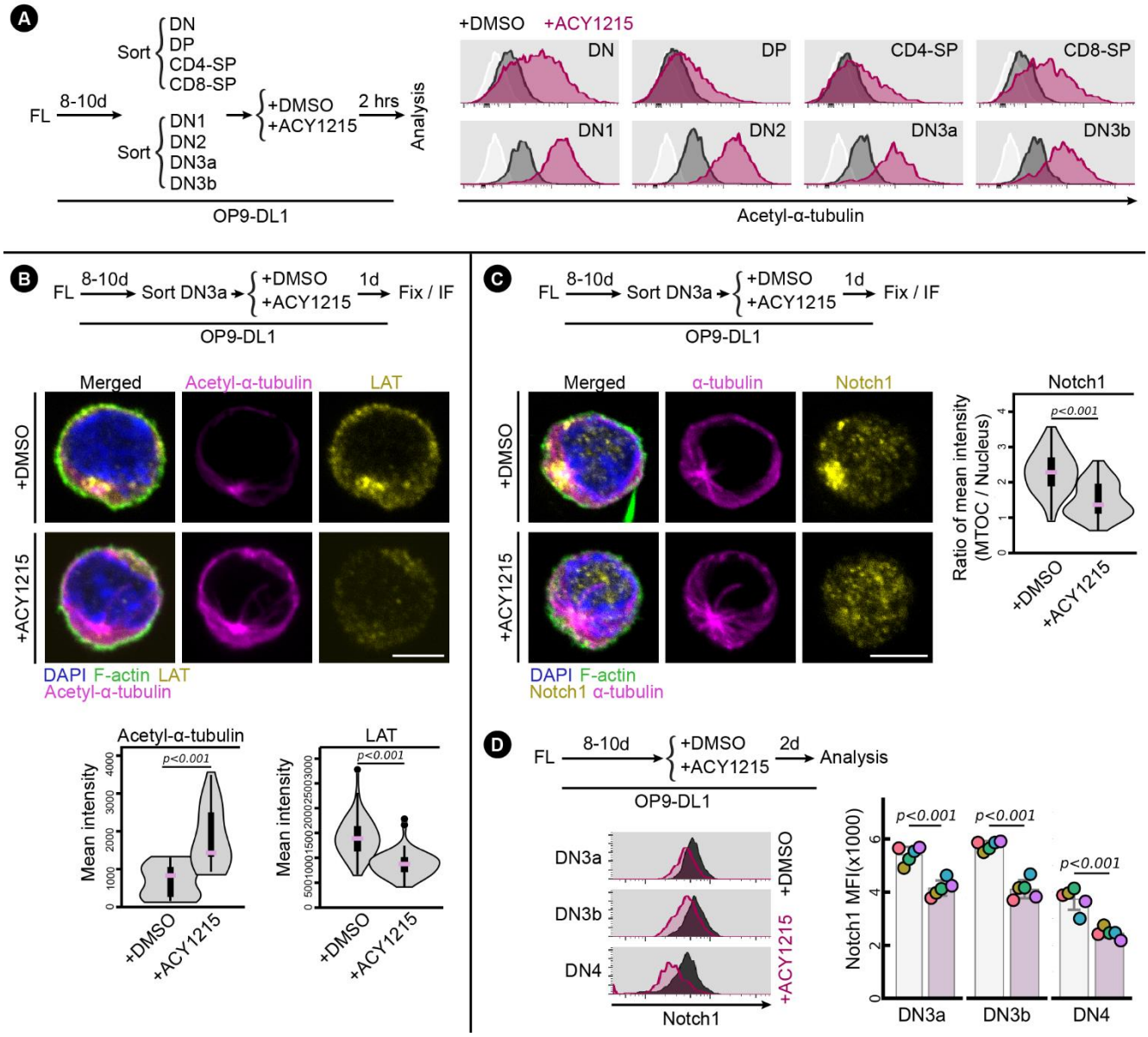
A
FL
8-10d
Sort
DN
DP
CD4-SP
CD8-SP
Sort
DN1
DN2
DN3a
DN3b
+DMSO
+ACY1215
2 hrs
Analysis
OP9-DL1
+DMSO
+ACY1215
DN
DP
CD4-SP
CD8-SP
DN1
DN2
DN3a
DN3b
Acetyl-α-tubulin
B
FL
8-10d
Sort DN3a
+DMSO
+ACY1215
1d
Fix / IF
OP9-DL1
Merged
Acetyl-α-tubulin
LAT
+DMSO
+ACY1215
DAPI F-actin LAT
Acetyl-α-tubulin
Acetyl-α-tubulin
Mean intensity
p<0.001
+DMSO
+ACY1215
LAT
Mean intensity
p<0.001
+DMSO
+ACY1215
C
FL
8-10d
Sort DN3a
+DMSO
+ACY1215
1d
Fix / IF
OP9-DL1
Merged
α-tubulin
Notch1
+DMSO
+ACY1215
DAPI F-actin
Notch1 α-tubulin
Notch1
Ratio of mean intensity
(MTOC / Nucleus)
p<0.001
+DMSO
+ACY1215
D
FL
8-10d
+DMSO
+ACY1215
2d
Analysis
OP9-DL1
DN3a
DN3b
DN4
+DMSO
+ACY1215
Notch1
Notch1 MFI(x1000)
p<0.001
p<0.001
p<0.001
DN3a
DN3b
DN4

Figure 6.

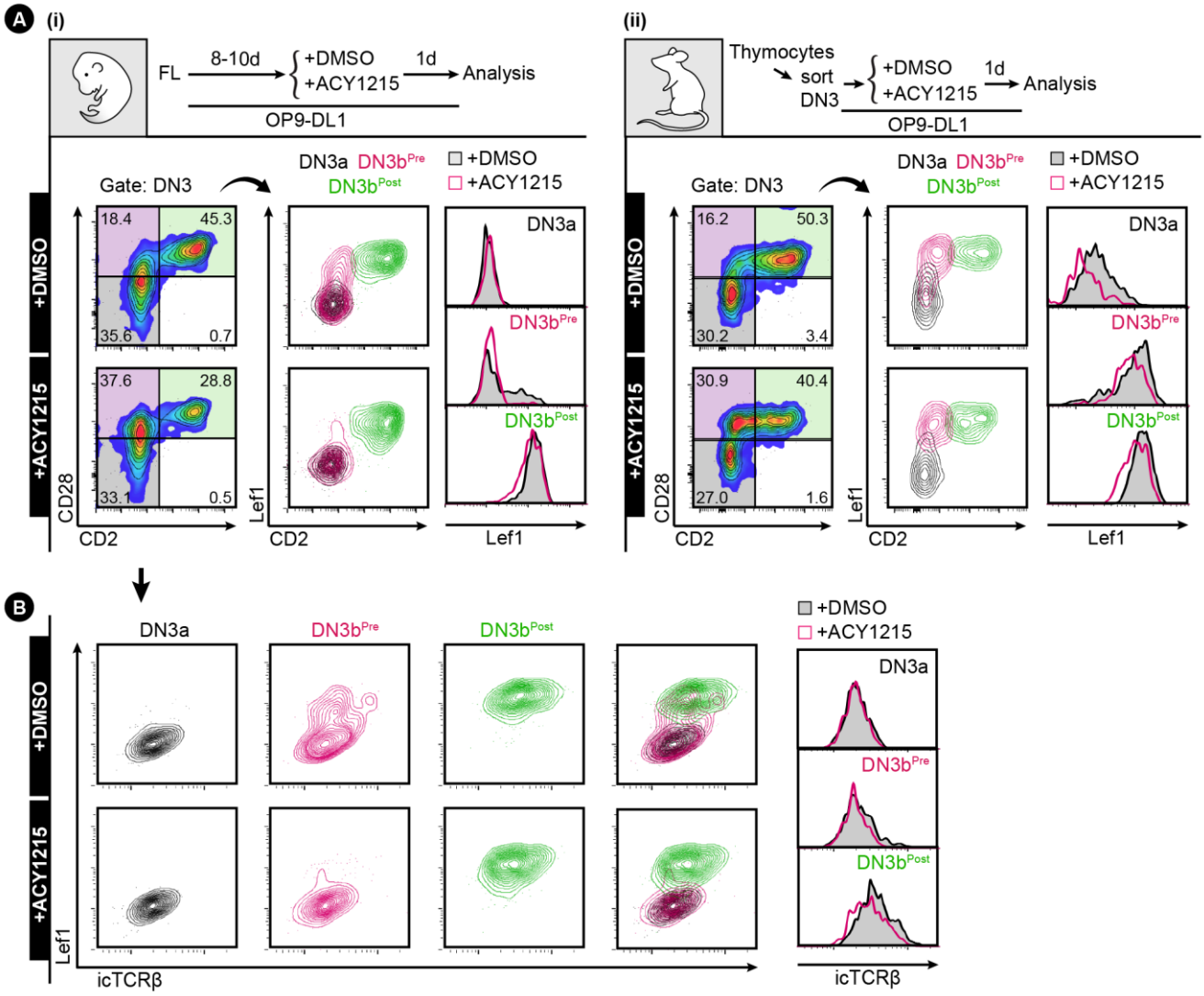
A
(i)
FL
8-10d
+DMSO
+ACY1215
1d
Analysis
OP9-DL1
Gate: DN3
DN3a
DN3b^Pre
DN3b^Post
+DMSO
+ACY1215
18.4
45.3
35.6
0.7
37.6
28.8
33.1
0.5
CD28
CD2
Lef1
(ii)
Thymocytes
sort
DN3
16.2
50.3
30.2
3.4
30.9
40.4
27.0
1.6
B
icTCRβ

Figure 7.

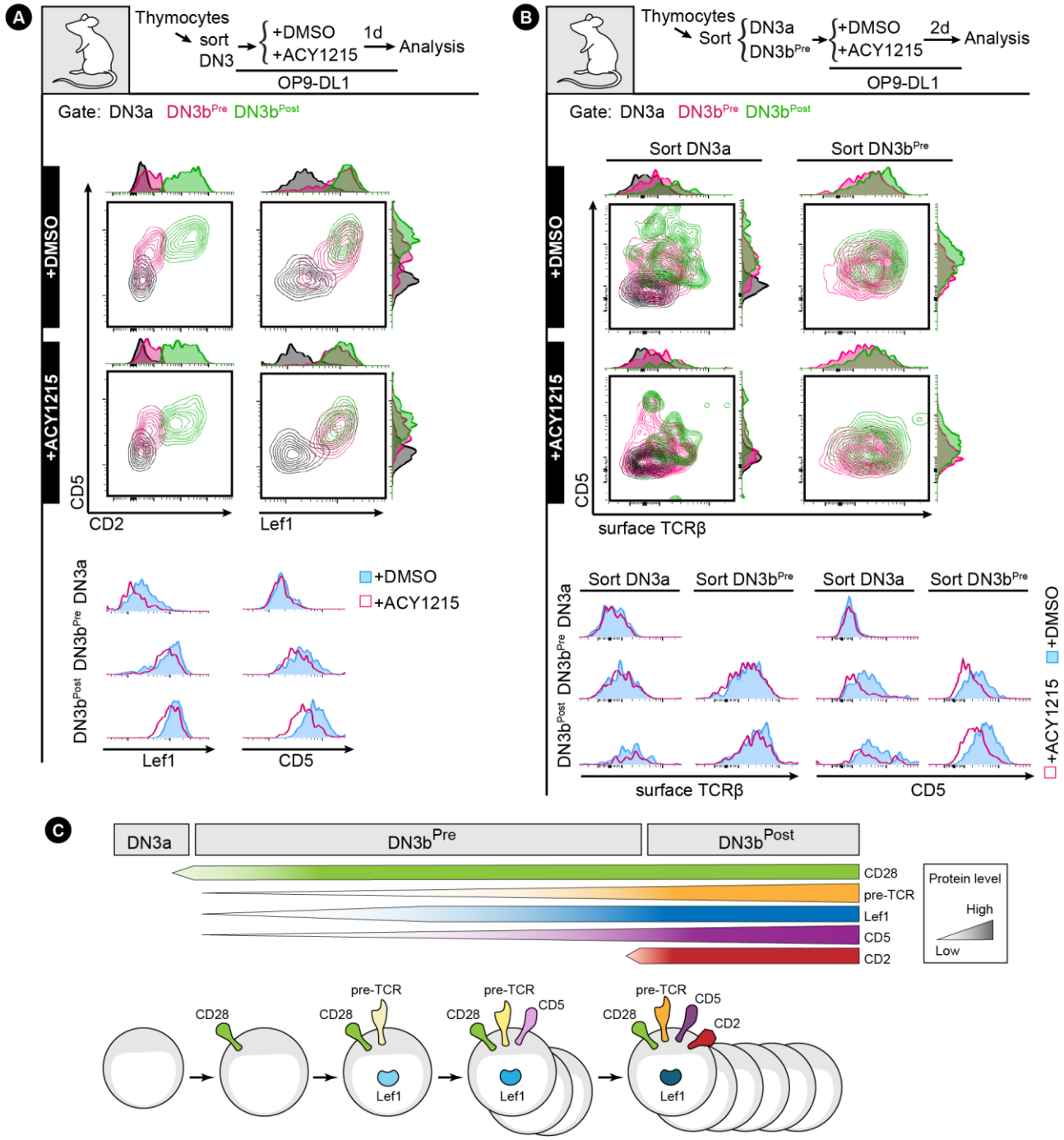

Chann et al. TCR co-receptors are expressed sequentially to fine-tune early αβ T cell development

Figure 8.

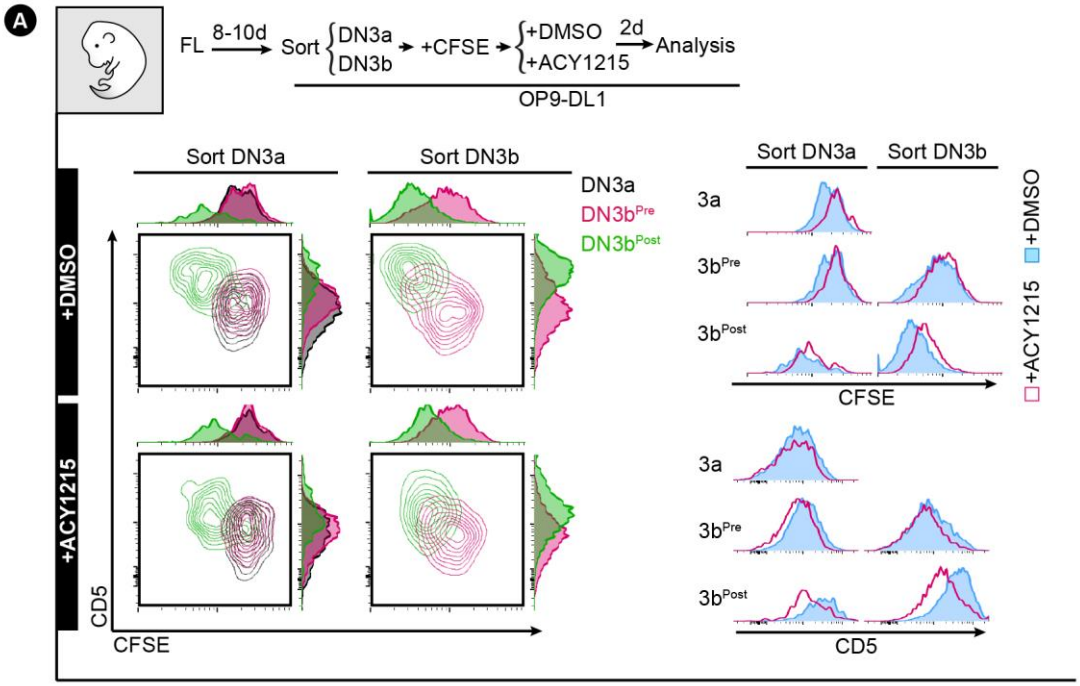
A
FL
8-10d
Sort
DN3a
DN3b
+CFSE
+DMSO
+ACY1215
2d
Analysis
OP9-DL1
Sort DN3a
Sort DN3b
DN3a
DN3b^Pre
DN3b^Post
+DMSO
+ACY1215
CD5
CFSE
3a
3b^Pre
3b^Post
CFSE
CD5
+DMSO
+ACY1215

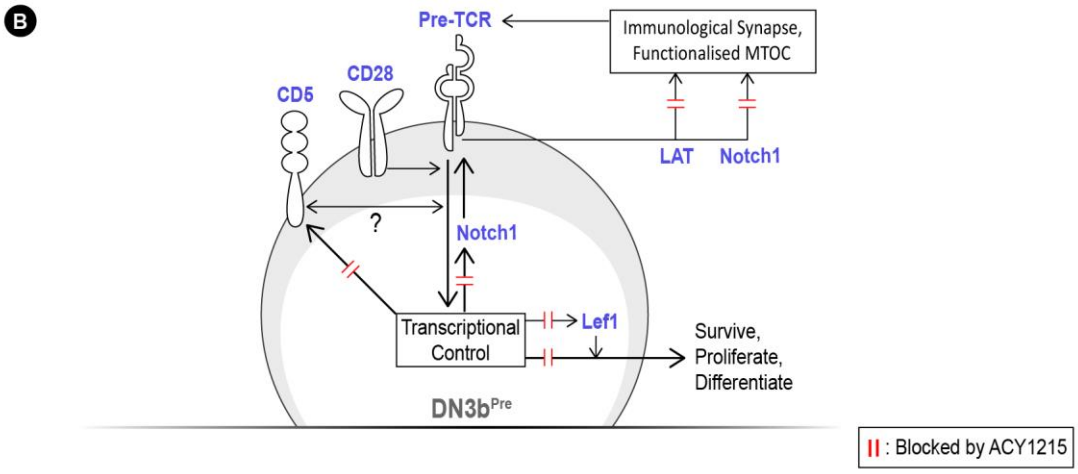
B
Pre-TCR
Immunological Synapse, Functionalised MTOC
CD28
CD5
LAT
Notch1
?
Notch1
Transcriptional Control
Lef1
Survive, Proliferate, Differentiate
DN3b^Pre
: Blocked by ACY1215

Supplementary Figure 1

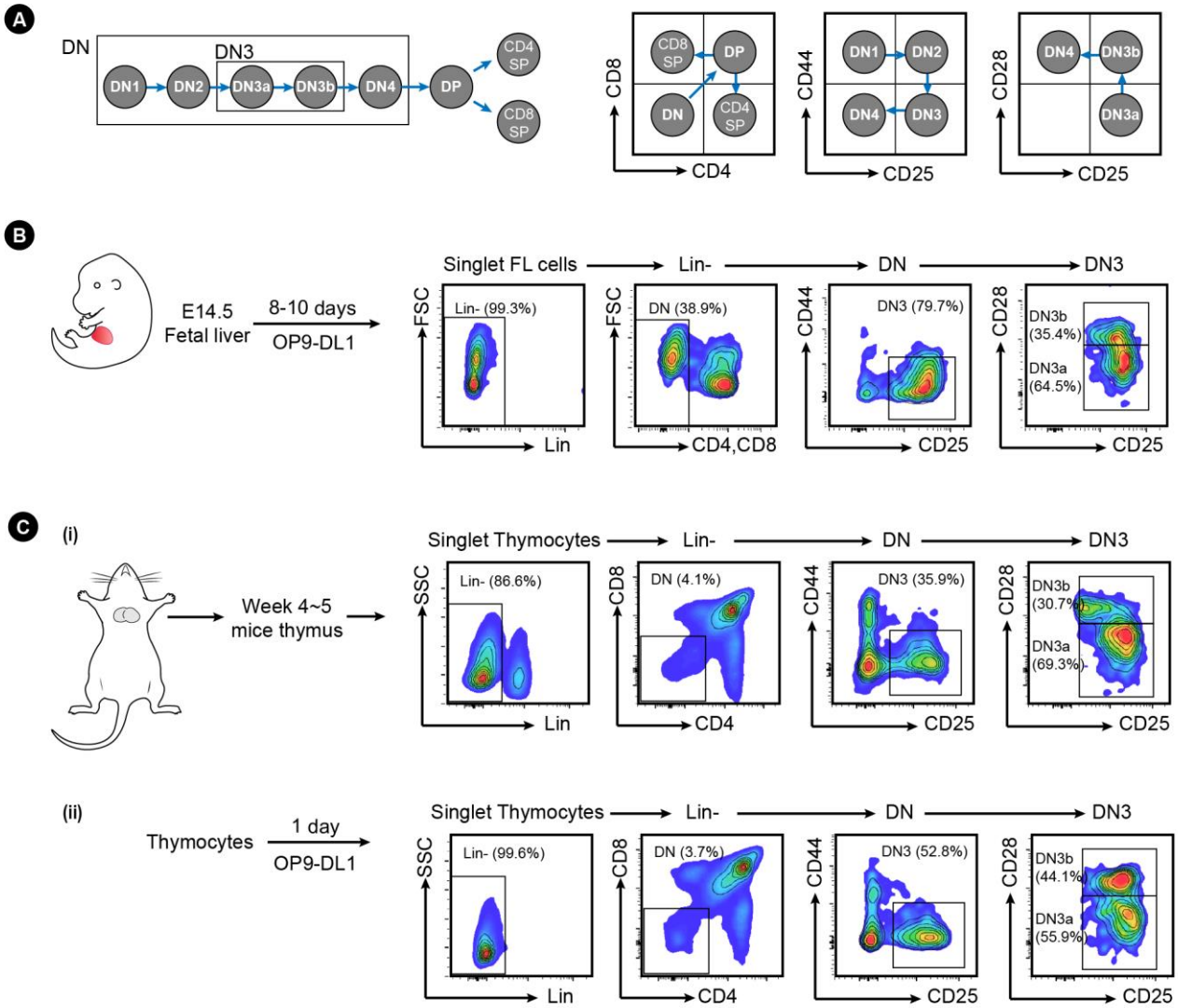

Supplementary Figure 2

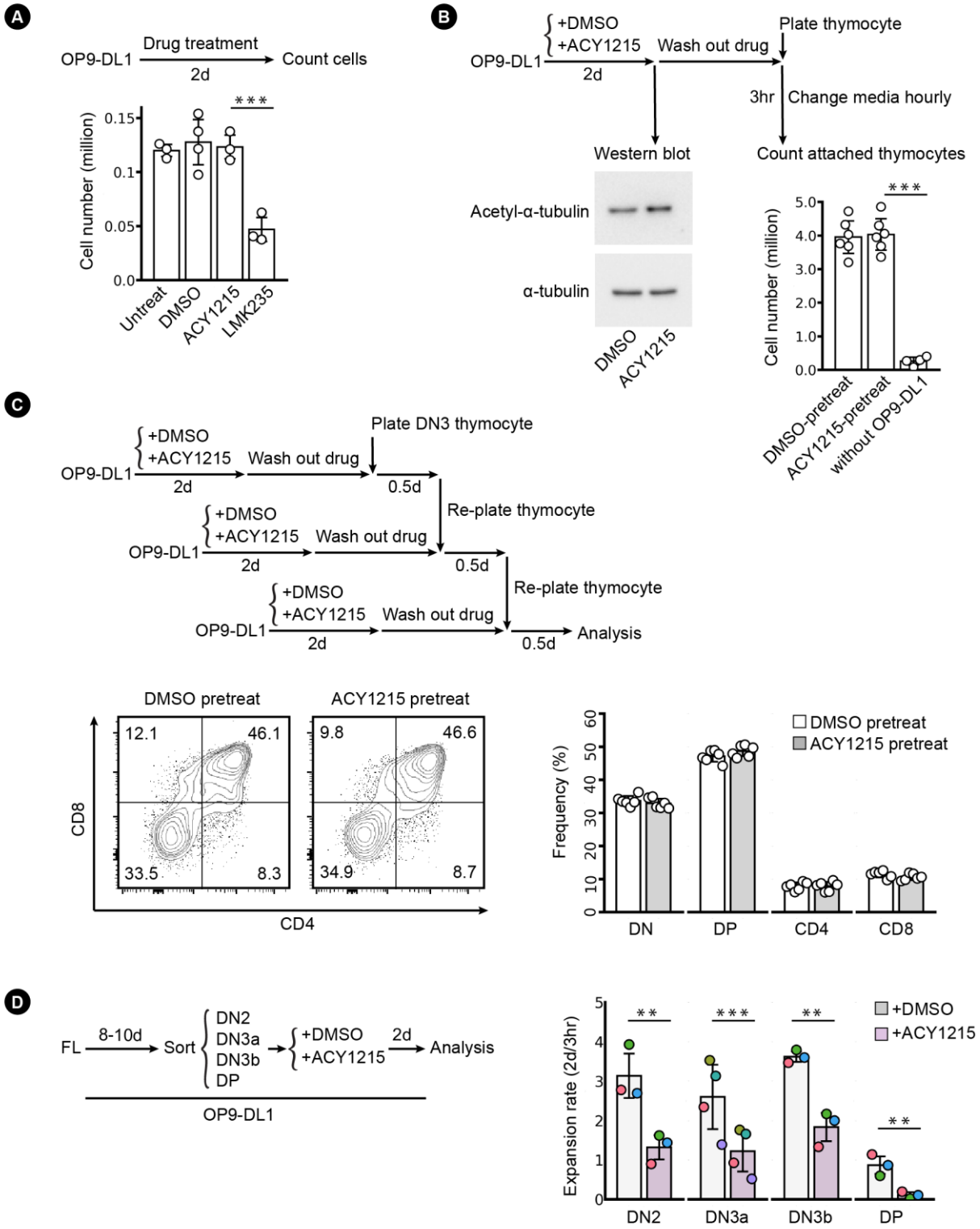

Supplementary Figure 3

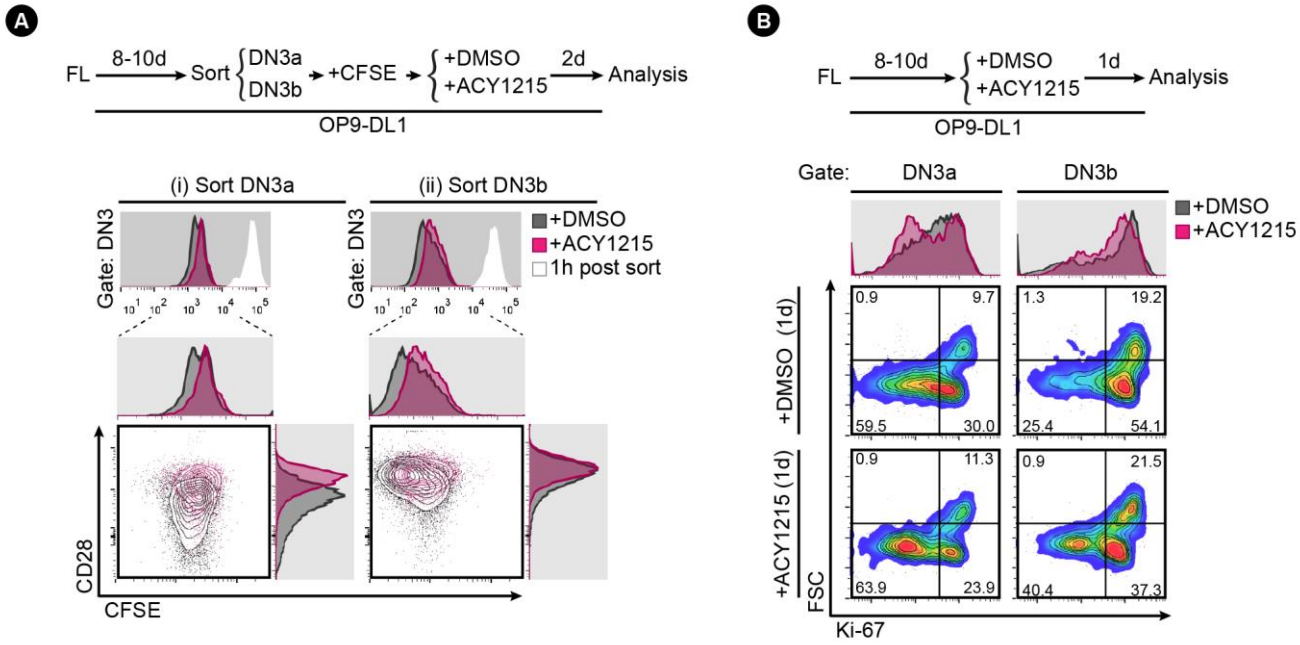

Supplementary Figure 4

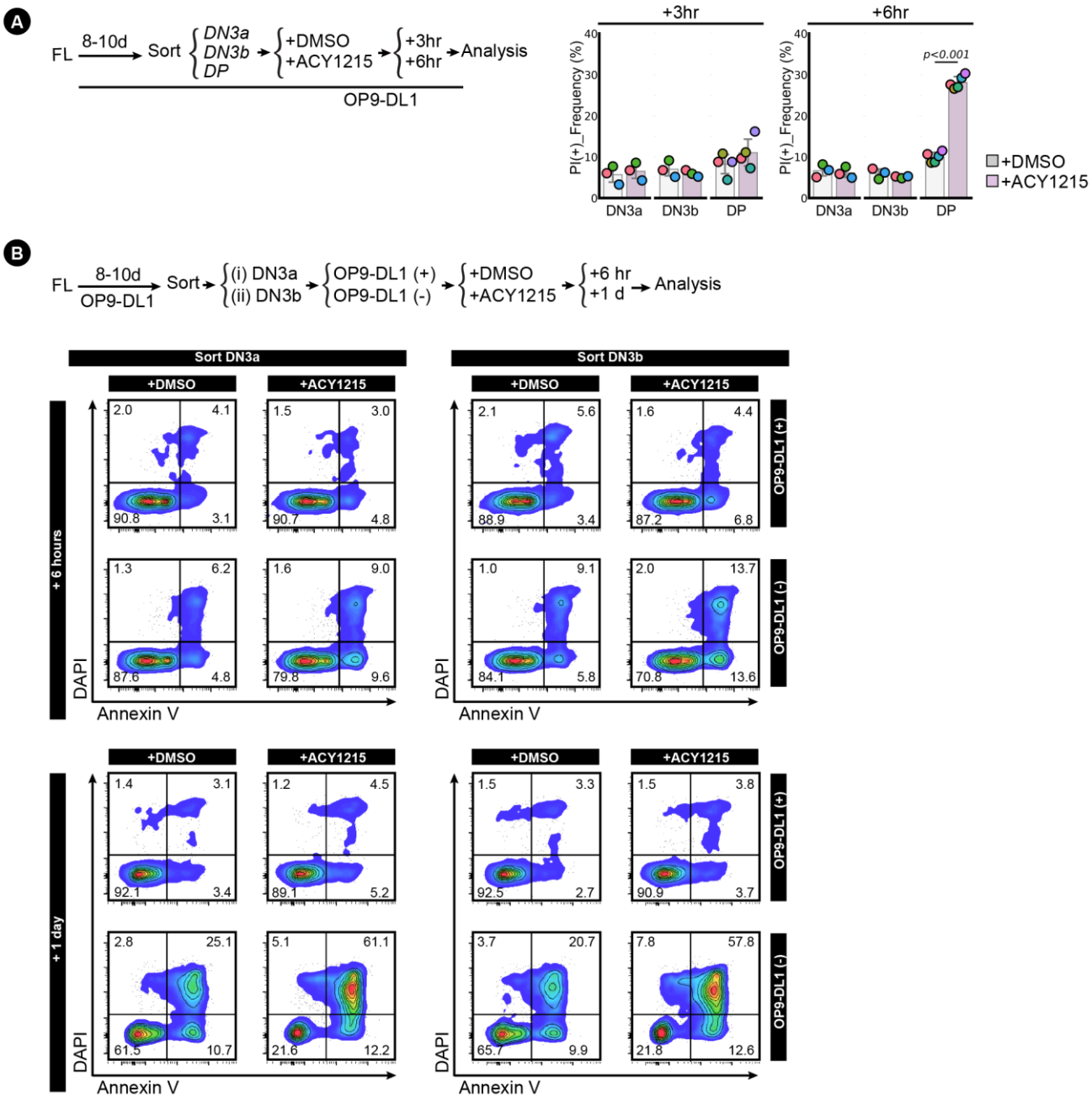

Supplementary Figure 5

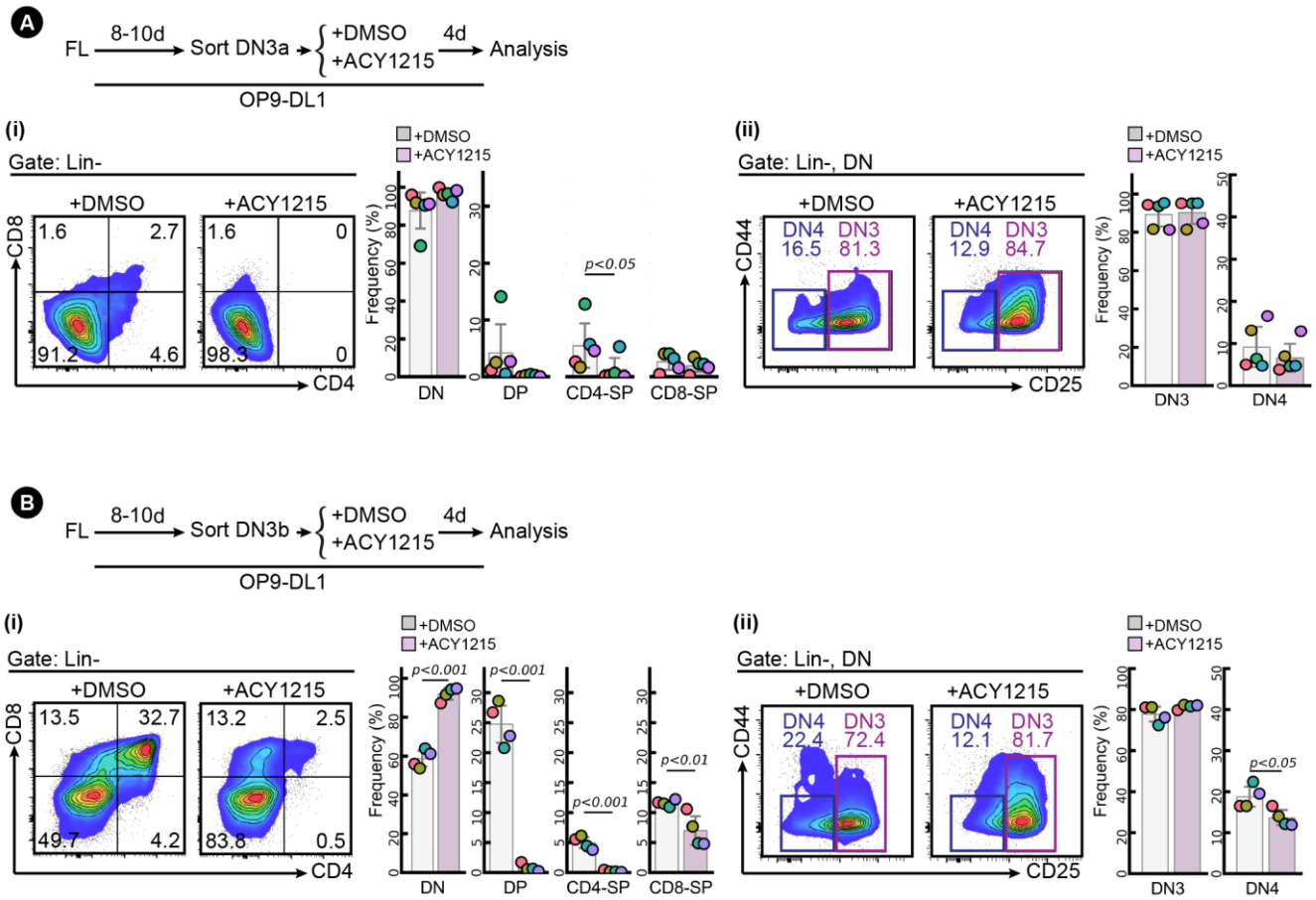

Supplementary Figure 6

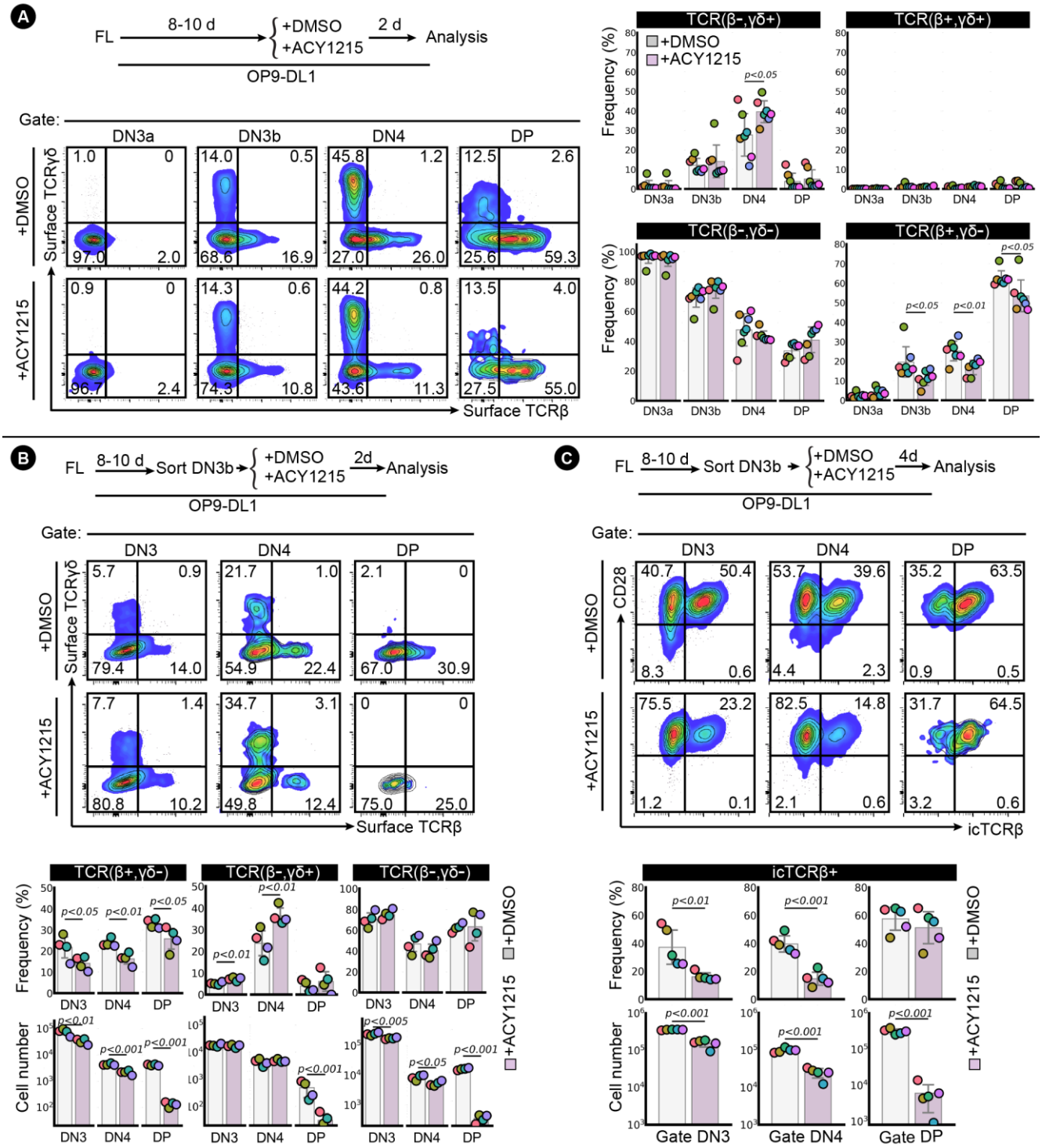

Supplementary Figure 7

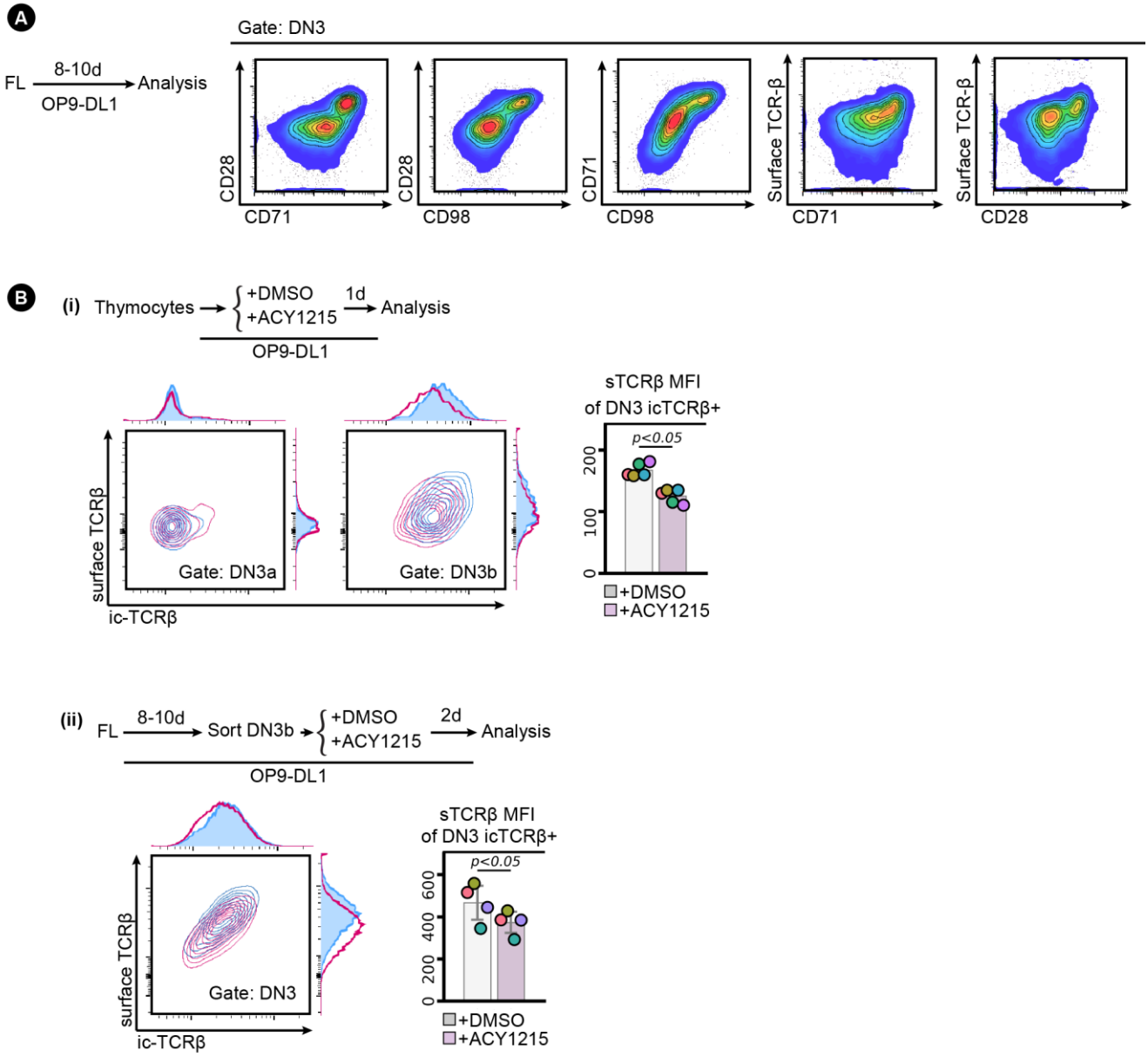

Supplementary Figure 8

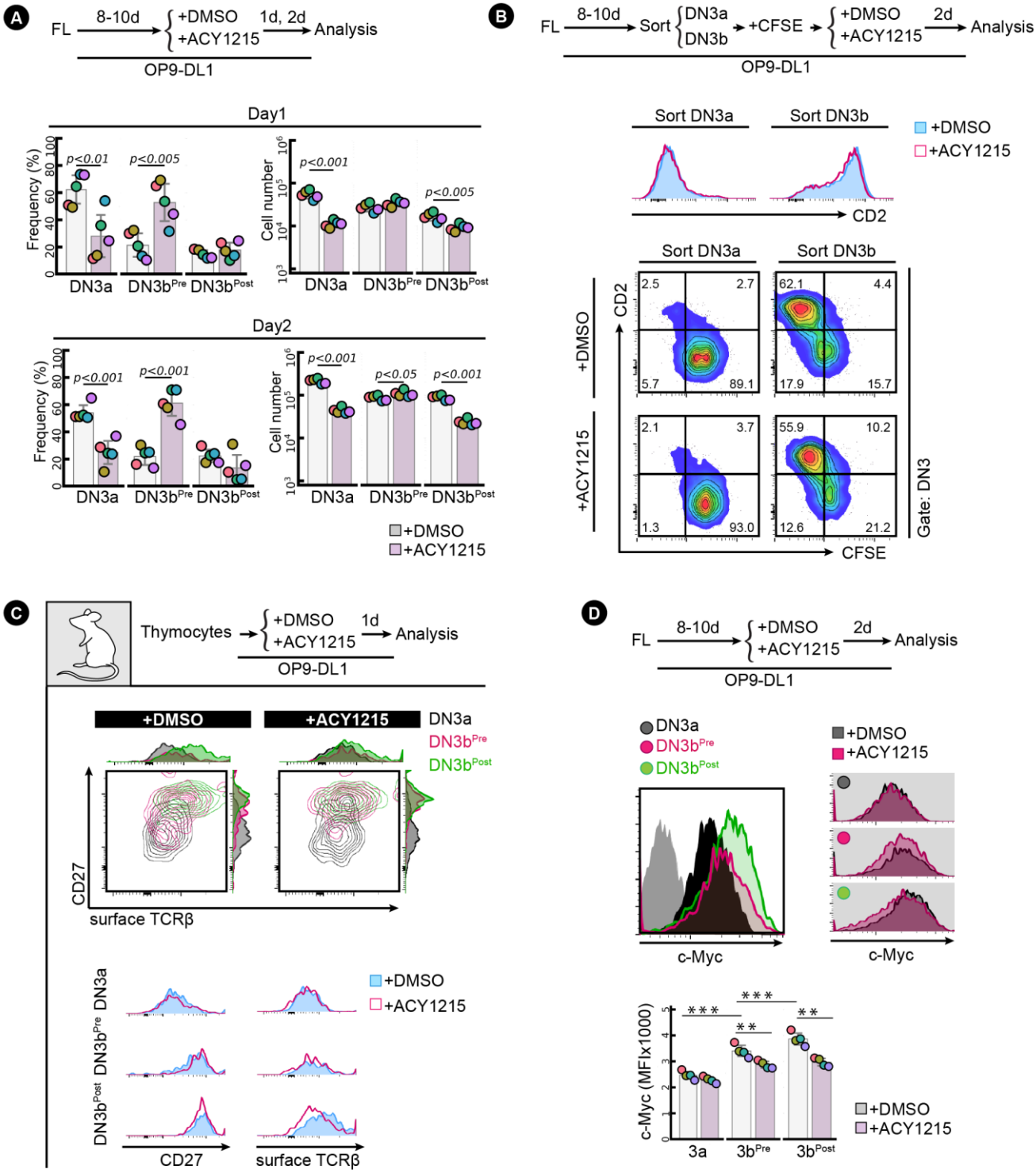

Supplementary Figure 9

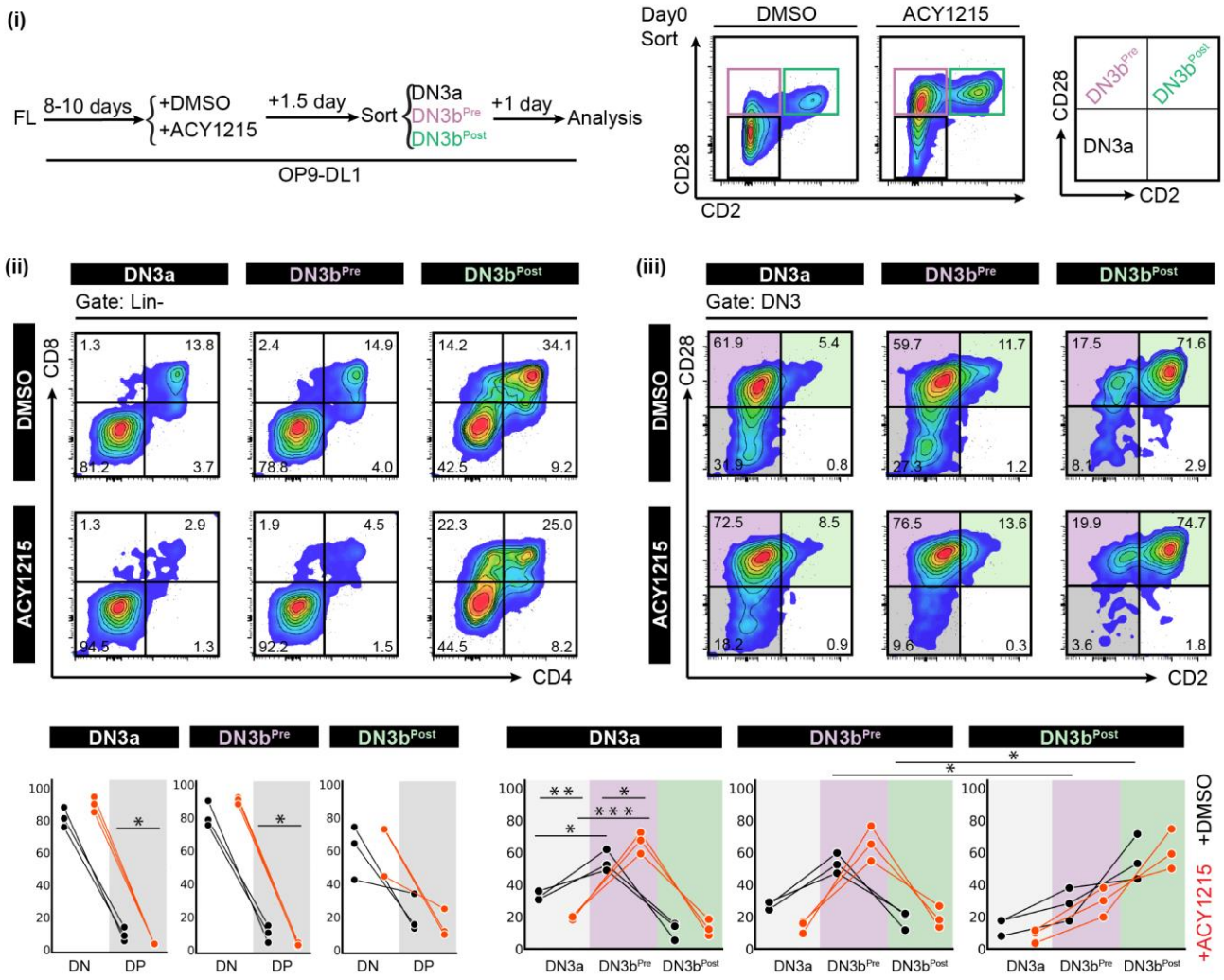

Supplementary Figure 10

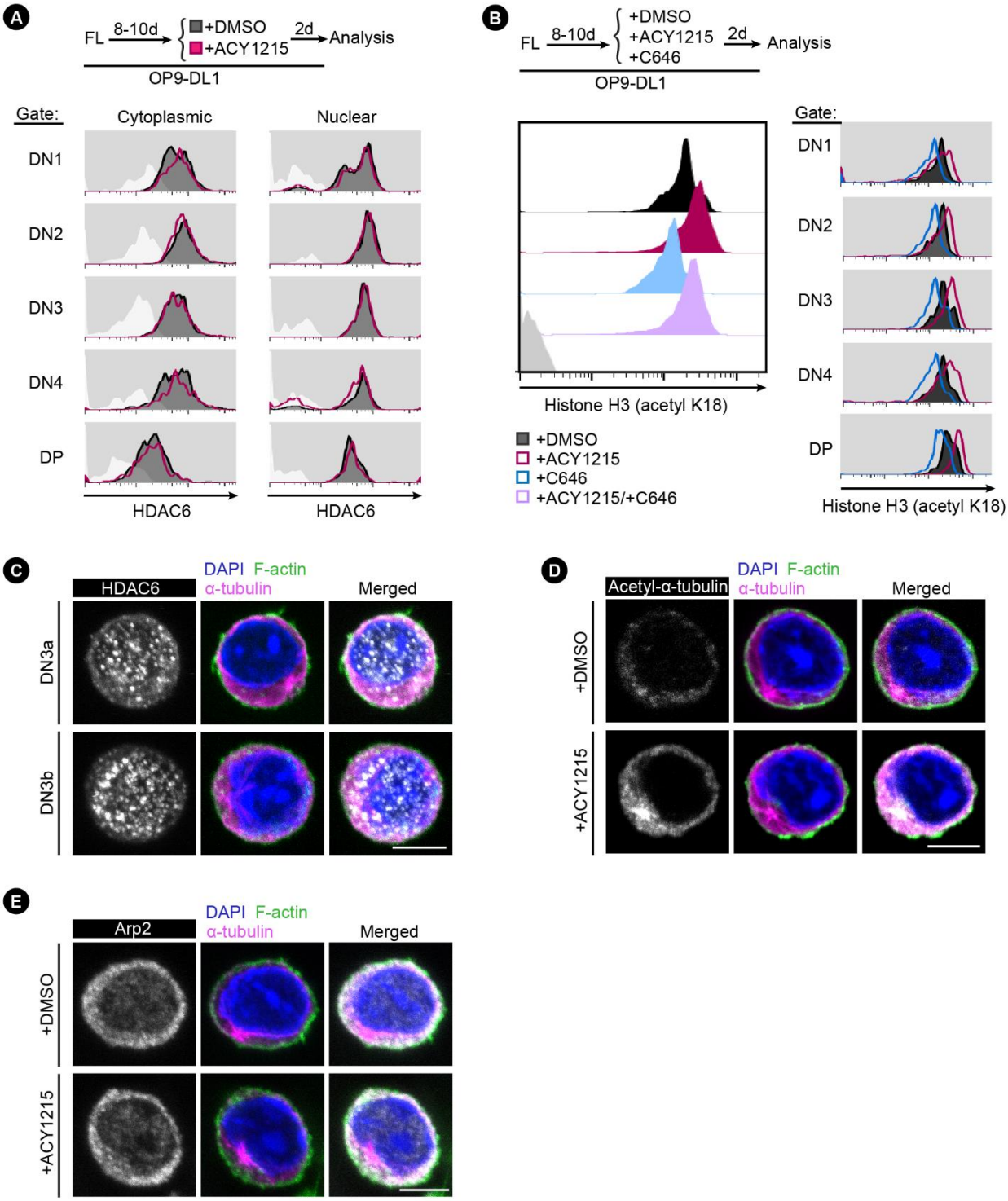

Supplementary Figure 11

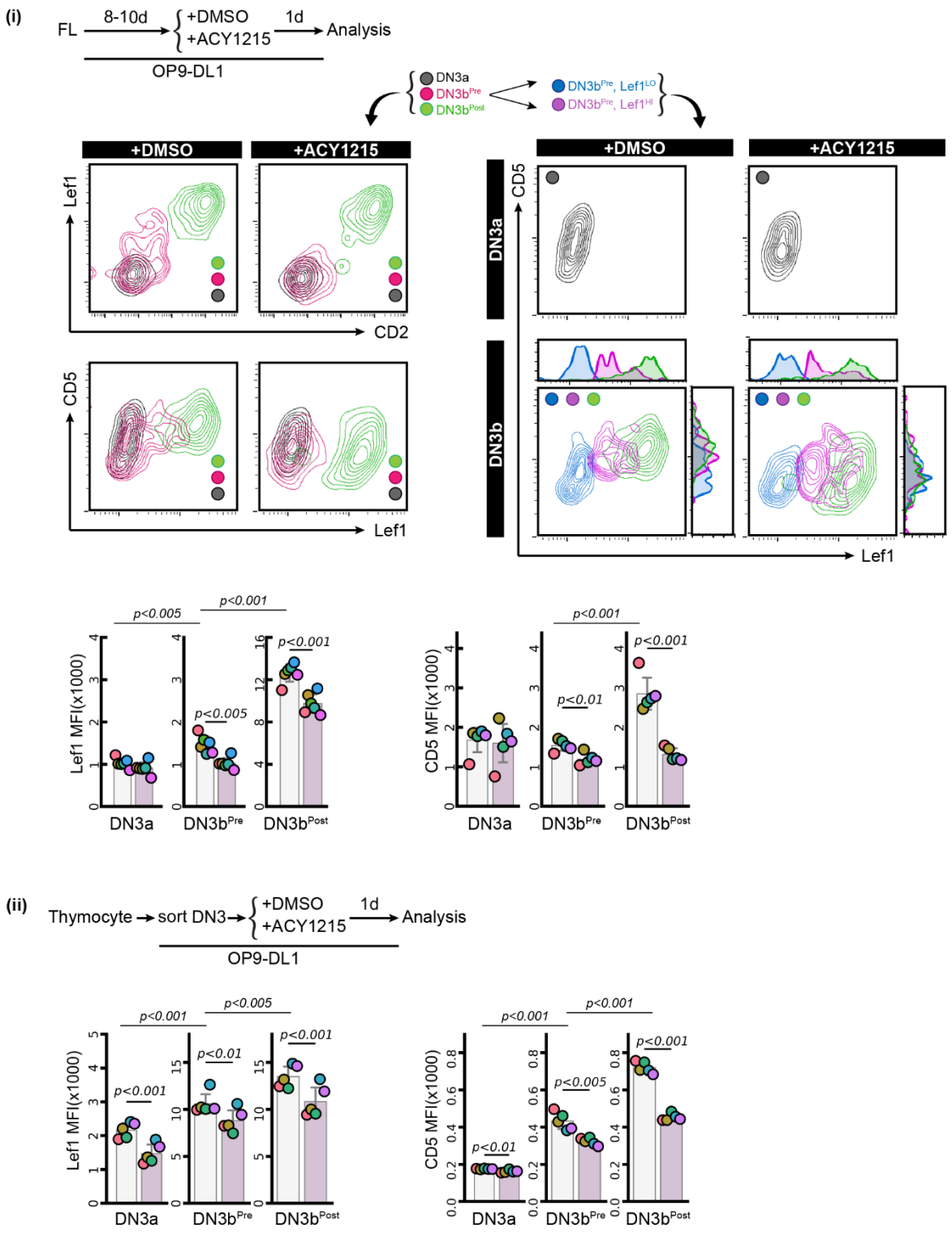

Supplementary Figure 12

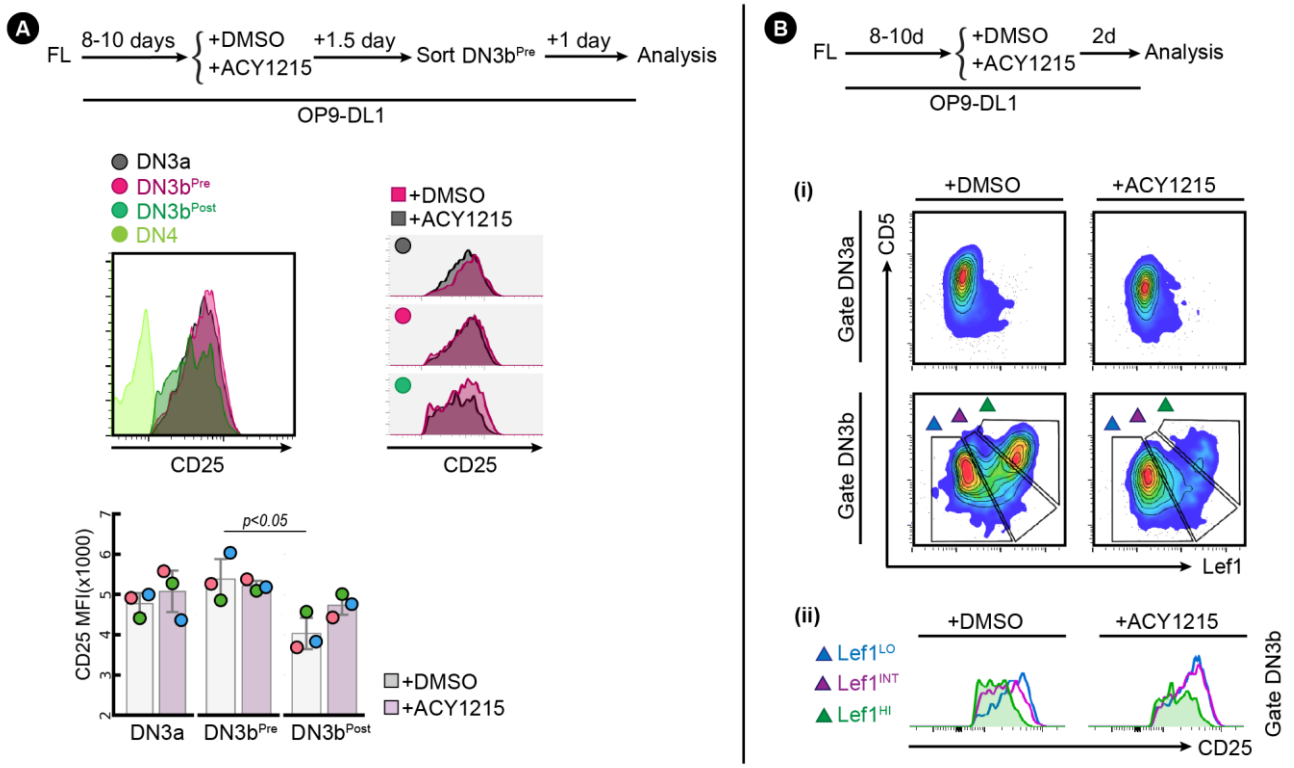

Supplementary Figure 13

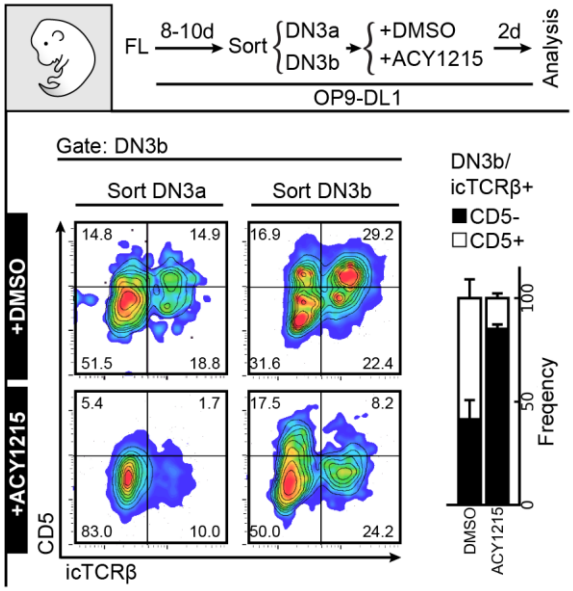

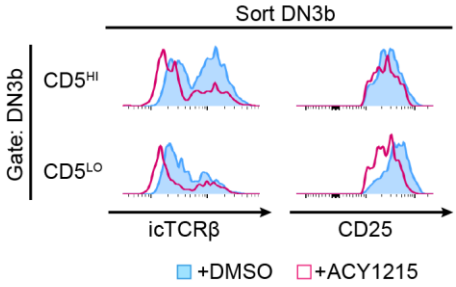
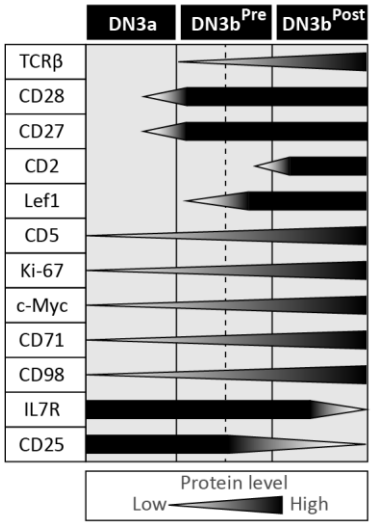
Supplementary Figure 14